Title
Climate controls on ecosystem production, biomass, and water cycling

Author
Kelly, Anne E.

Publication Date
2014

UNIVERSITY OF CALIFORNIA,
IRVINE

Climate controls on ecosystem production, biomass, and water cycling

DISSERTATION

Submitted in partial satisfaction of the requirements
for the degree of

DOCTOR OF PHILOSOPHY

in Earth System Science

by

Anne E. Kelly

Dissertation committee:
Professor Michael Goulden, Chair
Professor Claudia Czimczik
Professor James Randerson

2014

TABLE OF CONTENTS

LIST OF FIGURES iv
LIST OF TABLES vii
ACKNOWLEDGEMENTS viii
CURRICULUM VITAE x
ABSTRACT OF THE DISSERTATION xii
Chapter 1. Introduction 1

    Outline of the dissertation 3

Chapter 2. Limits on woody biomass and production along a 2300 m elevation gradient 5

    2.1. Introduction 6

    2.2. Methods 7

    2.3. Results 15

    2.4. Discussion 25

Chapter 3. A montane Mediterranean climate supports year round growth and high biomass 31

    3.1. Introduction 32

    3.2. Methods 33

    3.3. Results 38

    3.4. Discussion 47

Chapter 4. Water use efficiency variability and controls across ten California ecosystems 53

    4.1. Introduction 53

    4.2. Methods 54

    4.3. Results and Discussion 56

    4.4. Conclusions 64

Chapter 5. Conclusions 65

    5.1. Chapter synopses 65

    5.2 Implications and future directions 66

Bibliography 68

LIST OF FIGURES

Figure 2.1. Diagnostic framework for controls on aboveground woody biomass. Paralellograms are fluxes, boxes are pools, and circles are controls on fluxes. 7

Figure 2.2. Photos of the four sites in summer 2010. a) Oak savannah at 405 m, b) Ponderosa forest at 1165 m, c) Sierra mixed conifer forest at 2015 m, d) Lodgepole forest at 2700 m.......... 9

Figure 2.3. Site layout on LANDSAT false color (5-4-3). 11

Figure 2.4.Annual water year weather and water balance at the four sites: a) growing degree days, b) potential evapotranspiration, c) precipitation, d) “water balance” = precipitation – PET. 16

Figure 2.5. Aboveground biomass (tC ha^{-1}).. 17

Figure 2.6. Carbon fluxes (tC ha^{-1} yr^{-1}). a) GPP, b) ANPP. Solid fill is stem production, stippled fill is leaf production. 18

Figure 2.7. Growing season properties. a) growing season length, b) mean daily growing season GEE, c) growing season fPAR.. 20

Figure 2.8. Aboveground carbon use efficiency. 21

Figure 2.10. Aboveground woody carbon turnover times, τ_w. 23

Figure 3.1. Plot layout and location within California. Inset image is LANDSAT ETM+ bands 5-4-3 (August 2002). Right image is a NSF NCALM LiDAR image (July 2010) with hillslope and tree shading. 34

Figure 3.2. Stand demographics in September 2008, including all trees with dbh > 10 cm within the 1 ha plot... 35

Figure 3.3. Weather in water year 2010. a) Daily high (close circles) and low (open circles) air temperatures measured at the tower top (^{0}C), b) daily total incoming solar radiation (MJ m-2 d-1), c) daily high and low vapor saturation deficit (kPa), and d) cumulative precipitation (mm). 39

Figure 3.4. Air temperature at 2 m, 10 m, 25 m, and 55 m above ground level during the day (solid lines) and at night (dashed lines) during a) winter (DJF) and b) summer (JJA). Error bars are standard errors of the means. 40

Figure 3.5. Seasonal carbon exchange from 2009 – 2012 in tC [3 mo]$^{-1}$. a) Gross ecosystem exchange, b) respiration, and c) aboveground net primary production. 41

Figure 3.6. Cumulative carbon and water exchange from September 2009 to September 2012. a) GEE (solid line) and ANPP (dashed line), b) ET (solid line) and precipitation (dashed line). 42

Figure 3.7. GEE response to temperature by season. Temperature is binned in 2^{0}C increments, minimum 20 points per bin. 43

Figure 3.8. Seasonal water exchange. a) Total seasonal evapotranspiration (mm H_2O), dotted line is mean seasonal PET, b) mean seasonal water use efficiency during sunny periods (K > 600 W m^{-2}), c) total seasonal precipitation (mm H_2O). 44

Figure 3.9. Mean seasonal grams of gross carbon uptake per incoming megajoule of solar radiation. 45

Figure 4.1. Ecosystem water use efficiency, gross primary production, and evapotranspiration with respect to annual precipitation. Thin lines are linear fits of variables vs. annual precipitation at each site. Bold lines are inverse exponential fits to all sites excluding lodgepole forest. a) Annual water use efficiency (WUE; mmol CO_2 [mol H_2O]$^{-1}$). b) Gross primary production in tC ha^{-1}. c) Evapotranspiration in mm yr^{-1}. 57

Figure 4.2. Surface evaporation. a) Annual WUE as a function of fraction of ET lost to surface evaporation. b) Surface evaporation fraction of ET as a function of annual precipitation. 59

Figure 4.3. Annual WUE vs. VPD (kPa) weighted by half-hourly GEE during sunny periods (K > 400 m^{-2}). 60

Figure 4.4. WUE vs c_i/c_a during sunny periods (K > 400 W m^{-2}) with moderate VPD (0.5 - 3.0 kPa). 62

LIST OF TABLES

Table 2.1. Site characteristics. 10

Table 2.2. Weather means for WY 2009-2012. 10

Table 2.3. Biomass in a 1 ha plot around each tower site and date first measured. Top three dominant species' biomasses are also listed, except in the lodgepole forest where only two species were present. 12

Table 2.4. Summary of control values in the diagnostic framework [Figure 2.1]. 24

Table 2.5. Summary of flux values in the diagnostic framework [Figure 2.1]. 24

Table 3.1. Weather at the tower site measured during water years 2008-12 (Sept. 1, 2007 – Aug. 31, 2012). 40

Table 4.1. Site ecosystem types, locations, mean annual temperature (MAT) and mean annual precipitation (MAP). 54

ACKNOWLEDGEMENTS

Thank you everyone who shared campfire stories and warm beer and whitethorn and melded mountain dust into skin. I cherish those of you who helped me to learn during my time in the Sierra to learn that one of the mountain people. Thank you Aaron Fellows, whose energy and fearlessness made the cliff-scrambles through manzanita a sincere pleasure, and whose curiosity often pulled me out of data quicksand. Thank you Paige Austin, who laughed and charged ahead through the hottest, snakiest days. Thank you all of those who helped to haul heavy gear across talus, took turns coring hardpan, and sang 80s pop in the valley heat: Matt Meadows, Ryan Johnson, Christine Hedge, Kyongho Son, Ryan Lucas, Branko Kerkez, Pete Hartsough, Armen Malazian, and Scot Parker. It was always a delight to see your inappropriate rental cars rolling into Glen Meadow.

Thank you Tom Chester, Nate Stephenson, and Steve Hart. Our too-rare conversations conveyed their genuine enthusiasm for science and taught me that excellent research and a happy life were not mutually exclusive. This knowledge pushed me through the toughest days, and without that inspiration, I would probably be a liftie in Colorado.

Thank you friends who have been supportive through my time at UCI, those who shared desert starlight, eight-hour meetings, and Anthill pitchers. Without them, I would have been derailed from my dissertation by much greater challenges. I am unable to express the depths of my gratitude here, but I hope I can return what you have given me.

Thank you Mike Goulden, my adviser, who gave me just enough rope and unknotted it at key moments with clear insights. His incisive scientific approach cut through the murkiest problems, and I would do well to gain a fraction of that ability.

Thank you to the funders who trusted my research ideas: the Jenkins family, the ARCS Foundation Orange County chapter, the NASA Earth and Space Science Fellowship, the NASA Space Grant, and the NSF Southern Sierra Critical Zone Observatory. Every day I have been thankful for the privilege of support for the work I truly love.

CURRICULUM VITAE

Anne E. Kelly

Education

2014 PhD, University of California, Irvine: Irvine, CA; Earth System Science

Dissertation title: “Climate controls on ecosystem production, biomass, and water cycling”

2011 MS, University of California, Irvine: Irvine, CA; Earth System Science

2007 MS, California State University, Los Angeles: Los Angeles, CA; Environmental Science

Thesis title: “Shifts in the Deep Canyon Ecocline, 1977-2007”

2001 B.S., California Institute of Technology: Pasadena, CA; Physics

Work Experience

2008-2014 Graduate student researcher, University of California, Irvine: Irvine, CA

2010-2012 Teaching assistant, University of California, Irvine: Irvine, CA

2008 Teaching assistant, University of Toronto: Toronto, ON, Canada

2005-2007 Graduate student researcher, California State University, Los Angeles: Los Angeles, CA

2005-2006 Science teacher, Franklin High School: Los Angeles, CA

2001-2007 Applications developer, Infrared Processing and Analysis Center: Pasadena, CA

Peer-reviewed publications

Kelly, A. E. (2013). Vegetation Distribution Shifts. In T. Kadir, L. Mazur, C. Milanes, & K. Randles (Eds.), *Indicators of Climate Change in California* (2013 ed., pp. 157–163). Sacramento, CA: California Environmental Protection Agency, Office of Environmental Health Hazards Assessment.

Goulden, M. L., Anderson, R. G., Bales, R. C., **Kelly, A. E.**, Meadows, M., & Winston, G. C. (2012). Evapotranspiration along an elevation gradient in California's Sierra Nevada. *Journal of Geophysical Research*, *117*(G3), 1–13.

Trujillo-Gomez, E., Molotch, N. P., Goulden, M. L., **Kelly, A. E.**, & Bales, R. C. (2012). Elevation-dependent influence of snow accumulation on forest greening. *Nature Geoscience*, *5*(10), 705–709. doi:10.1038/ngeo1571

Kelly, A. E., & Goulden, M. L. (2008). Rapid shifts in plant distribution with recent climate change. *Proceedings of the National Academy of Sciences of the United States of America*, *105*(33), 11823–6.

ABSTRACT OF THE DISSERTATION

Climate controls on ecosystem production, biomass, and water cycling

by

Anne E. Kelly

Doctor of Philosophy in Earth System Science

University of California Irvine, 2014

Professor Michael Goulden, Chair

The association between climate and vegetation distribution has long been acknowledged, but quantifying the limits of climate on vegetation growth, biomass, and mortality remains an unsolved problem. Accurate prediction of the effects of climate change requires an understanding of the physiological limitations on vegetation due to climate. Recent increases in forest mortality and wildfire in Western North America has been attributed to warming and drought, but the causal mechanisms have not been identified. This dissertation uses observations of weather and vegetation growth, biomass, and water use to compare diverse ecosystems' responses to temperature and water availability and identify physiological thresholds that could promote ecosystem resilience or vulnerability to climate change.

The first chapter constructs a diagnostic framework of climatic control on biomass. The study system was the western slope of the Sierra Nevada Mountains of California. Climatic limitations on growth rates and growing seasons were compared across the gradient, along with ecosystem growth, death, and biomass. A broad "sweet spot" of climate conditions was found, in which winter cold and summer drought were minimal enough to allow a year-round growing season. Outside of this favorable zone, the combination of growing season lengths and mortality rates produced a low-biomass, fast-growing savannah at the lowest elevation and a high-biomass, slow-growing lodgepole forest at the highest elevation.

The second chapter examines the mixed conifer forest within the “sweet spot”. Two adaptations were identified to allow this forest to maintain year-round growth. First, photosynthesis rates were near maximum even as air temperatures dropped to freezing; this was a lower optimal temperature range than almost any other known forest. Second, this forest largely avoided moisture stress by accessing soil water throughout the summer drought period.

The third chapter explores relationships between annual precipitation and water use efficiency across ten diverse California ecosystems. The driest ecosystems exhibited low water use efficiency that varied with annual precipitation. Ecosystem water use efficiency at the dry sites responded to variable annual precipitation through increased surface evaporation, high vapor pressure deficit, and high internal CO_2 concentrations. The wetter montane conifer sites showed little to no response of water use efficiency to dry years.

Chapter 1. Introduction

Understanding the effects of climate change on terrestrial ecosystems is a critical problem for predicting terrestrial feedbacks to climate change as well as the future of ecosystem services. Warming temperature is not the only component of future climate change; changes in the water cycle are expected to occur, with intensification of precipitation and drought [*Huntington*, 2006]. There is evidence that other meteorological conditions will continue to change, including snowmelt timing [*Stewart et al.*, 2005], humidity, and cloud cover [*Roderick and Farquhar*, 2002]. The interacting effects of these complex changes are expected to produce novel climates that will affect ecosystem function and distribution [*Williams and Jackson*, 2007; *Williams et al.*, 2007].

Weather affects plant physiology in complex ways. Warming may increase photosynthesis rates, but may also increase respiration and ultimately lead to net carbon loss [*Piao et al.*, 2008]. Changes in amount and timing of precipitation may induce drought stress, leading to more frequent occurrences of the widespread drought seen across western North America at the turn of the 21st century [*Allen et al.*, 2010]. Some ecosystems will be more vulnerable and others more resilient to climate changes [*Parmesan*, 2006; *Scholze et al.*, 2006; *Bergengren et al.*, 2011]. Species ranges will contract with mortality or expand into newly favorable environments [*Loarie et al.*, 2008]. Different functional types will take over given regions [*Field et al.*, 2007]. These changes will alter ecosystem services, including feedbacks to the climate system including water cycling, albedo, and carbon storage [*Campbell et al.*, 2009]. Understanding physiological responses to climate changes, climate thresholds for species mortality, and differences in physiological adaptations to climate is critical for accurate prediction of future ecosystem function and terrestrial feedbacks to climate change.

Four main questions drove this research: 1) How does precipitation and temperature control biomass and gross primary production? 2) What are the physiological thresholds in drought limitation or cold limitation, and how do they vary across ecosystems? 3) What are some mechanisms of resilience to drought and cold limitations? 4) How does climate control ecosystem water use?

The theoretical approach of this research focuses on understanding the interactions of several fundamental ecosystem properties and meteorological variables using observations at a regional scale. Gross primary production (GPP), biomass, aboveground net primary production (ANPP), and evapotranspiration together define the most basic of ecosystem properties: growth, stature, and water use, which together govern ecosystem functional type [*Whittaker et al.*, 1973; *Whittaker and Niering*, 1975b]. Temperature, precipitation and their interaction are the definition of fundamental climate types [*Köppen*, 1884]. The link between Köppen-type climate classification and ecosystem functional type has long been acknowledged [*Merriam*, 1894; *Holdridge*, 1967; *Whittaker and Niering*, 1975b], but the mechanisms of climatological control on ecosystem function are still an area of active research and the focus of this dissertation.

This problem is being approached with global coupled models [*Medvigy et al.*, 2010], theoretical ecological modeling [*Guisan and Thuiller*, 2005], and observations [*Hinzman et al.*, 2005; *McDowell*, 2011; *Fellows and Goulden*, 2013]. Ground-based observations of meteorology and ecophysiological response are lacking at a spatial scale at which changes are likely to take place, i.e., across ecotones within potential range of future dispersal [*Jeschke and Strayer*, 2008]. Observations on this scale provide information not only about potential regional changes, but can elucidate patterns of ecosystem-level physiological response to climate that produce ecotones.

The general conceptual framework I use to investigate climate influence on ecosystem growth and function is partially outlined in Figure 2.1. This figure describes the basic ecologic controls on biomass. Gross primary production is limited both by growing season length and photosynthesis rates during the growing season. Carbon use efficiency determines how much photosynthetic carbon uptake is retained as net primary production. Ecosystem allocation to aboveground production governs aboveground net primary production. The rate of aboveground net primary production minus the rate of loss via vegetation mortality determines aboveground standing biomass. Altogether, this conceptual framework describes ecosystem functional type in terms of carbon cycling. Climate limitations on growing season length and photosynthesis rates via cold and drought limitation are the primary focus of two of the three research chapters. The final research chapter investigates how climate affects the interaction between gross primary production and evapotranspiration, or water use efficiency.

The methodological approach was a cross-spatio-temporal design, and took advantage of a suite of ten eddy covariance towers along two climate gradients in California. The first spanned 70 km west-to-east, ascending from 400 m in the San Joaquin Valley to a subalpine forest at 2700 m in the Sierra Nevada. The second spanned 100 km west-to-east, from coastal Southern California to the inland Mojave Desert. Observations were made on scales from minutes to years, so that both short- and long-term effects of weather on ecophysiology can be understood. Meteorology, CO_2 flux, H_2O flux, and heat fluxes were measured with the eddy covariance towers. Vegetation and soil moisture were monitored within the tower footprints.

Outline of the dissertation

The following chapters are an effort to answer the four overarching research questions previously listed. Chapter two explores the ecophysiological response of the Sierra gradient to weather and climate. Chapter three investigates how the large-statured trees of the Sierra mixed conifer forest are able to thrive in a summer-dry, snow-dominated climate. Chapter four separates out the major meteorological and ecophysiological controls on ecosystem water use efficiency across the ten tower sites in ten of California’s major ecosystems. Chapter five synthesizes the findings of the previous chapters and discusses future directions for research.

Chapter 2. Limits on woody biomass and production along a 2300 m elevation gradient

Abstract

Quantifying the climatic influence on ecosystem carbon and water cycling is a key problem for predicting terrestrial feedbacks to climate change. Temperature and precipitation interact in complex ways across a range of timescales to regulate photosynthetic rates, and ultimately ecosystem biomass and carbon storage. We used a 2300 m elevation gradient, from 405 m to 2700 m, in the Sierra Nevada Mountains of California to understand how climate controls photosynthetic rates, growing season length, and ecosystem biomass. Climatic relationships with gross primary production (GPP), carbon use efficiency (CUE), carbon allocation to wood, and carbon turnover time interacted to create an elevational distribution of biomass that peaked at mid-elevations. Carbon turnover time decreased and allocation to wood increased with decreasing temperature, and was a primary driver of the low-biomass foothill oak savannah and high-biomass subalpine lodgepole forest. These results emphasize the need for understanding ecosystem responses to climate to predict terrestrial carbon cycling and storage with future climate change.

2.1. Introduction

Climate is recognized as a primary external control on ecosystem type, range, biomass, and productivity [e.g. *Merriam*, 1894; *Whittaker and Niering*, 1975]. Climate does not control these ecosystem properties directly, but rather controls photosynthesis, respiration, and evapotranspiration (ET) rates. Climate-driven limits on vegetation physiology largely determine growing season, net primary production, and water stress. These physiological limitations favor some plant functional types over others in a given set of climate conditions, and produce distinct patterns of ecosystem types and carbon cycling across the landscape. Tree biomass, an important terrestrial carbon pool [*Dixon et al.*, 1994], is the balance between gross tree growth and tree mortality [*Stephenson et al.*, 2012]. Forest production and mortality, and thus biomass, have strong relationships with climate [e.g., *Whittaker and Niering*, 1975b; *Stephenson and Van Mantgem*, 2005; *Das et al.*, 2013].

There is growing concern that montane ecosystems are vulnerable to future warming and drought; recent evidence indicates that forest mortality rates in California's Sierra Nevada Mountains are already climbing due to recent climate change [*Van Mantgem and Stephenson*, 2007]. Potential impacts of drought and/or warming could include a combination of increased mortality [*Williams et al.*, 2012], biomass changes [*Fellows and Goulden*, 2012], and species distribution and range shifts [*Parmesan and Yohe*, 2003; *Millar et al.*, 2007; *Kelly and Goulden*, 2008; *Loarie et al.*, 2009]. Here, we investigated four sites spanning a 12^0C temperature and 600 mm precipitation gradient in the Sierra Nevada. We focus on three questions: 1) how and why do net primary production (NPP) and gross primary production (GPP) vary along the climate gradient? 2) how and why does biomass vary with elevation? and 3) what do these relationships predict about the ecological impact of potential climate change?

2.2. Methods

2.2.1. Conceptual and diagnostic framework

We constructed an observation-based diagnostic framework to understand the temperature and precipitation limitations on carbon cycling [Figure 2.1]. This framework predicts steady state woody biomass (or "carbon carrying capacity" as described by Keith et al. [2009]) given relationships between climatology and growing season, gross ecosystem exchange (GEE), carbon use efficiency, and carbon turnover time.

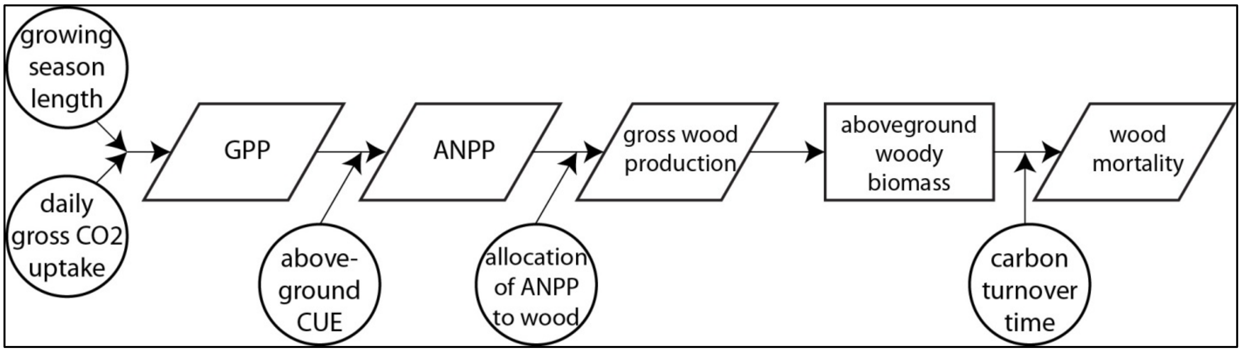

Figure 2.1. Diagnostic framework for controls on aboveground woody biomass. Paralellograms are fluxes, boxes are pools, and circles are controls on fluxes.

Woody biomass is a slow-turnover carbon pool, with a turnover time that is one to two orders of magnitude greater than herbs, grasses, foliage, and fine roots. Gross primary production can be described by the product of the growing season length and the rate of growth during the growing season. Growing season length can be truncated by drought stress and/or cold-induced dormancy. The rate of carbon uptake during the growing season is largely controlled by leaf area. Aboveground net primary production (ANPP) is a product of gross primary production and aboveground carbon use efficiency. Aboveground woody biomass production is the balance of ANPP not allocated to leaves. Both aboveground carbon use efficiency and wood:leaf allocation are associated with vegetation type, which is in turn associated with climate [*Walter and Breckle*, 2002]. This framework allows us to take the qualitative relationships between climate and biomass described by Merriam [1894] and Whittaker [*Whittaker and Niering*, 1975b] and make independent assessments of aboveground carbon pools under different climate conditions. We directly measured all the elements of our framework, and thus can analyze the sensitivity of each of the framework elements to changes in other elements.

The western slope of the Sierra Nevada Mountains is an ideal system to develop and test our conceptual framework. Chapin et al.'s extension [1996] of Jenny's state factor approach [1941] describes ecosystem structure and function as governed by five variables: climate, potential biota, topography, parent material, and time. Our study transect passes through oak savannah, ponderosa forest, mixed conifer forest, and subalpine lodgepole forest [Table 2.1]. The transect keeps four of Jenny's five factors as constant as possible, while the 2300 m elevation gain produces a gradient of temperature and precipitation [Table 2.2]. Potential biota is similar between sites, with the transect spanning just 65 km east-to-west and no barriers to species dispersal. Local topography of each site is gently rolling, with grades less than 3°. Parent material is granodiorite of the Sierra Nevada batholith.

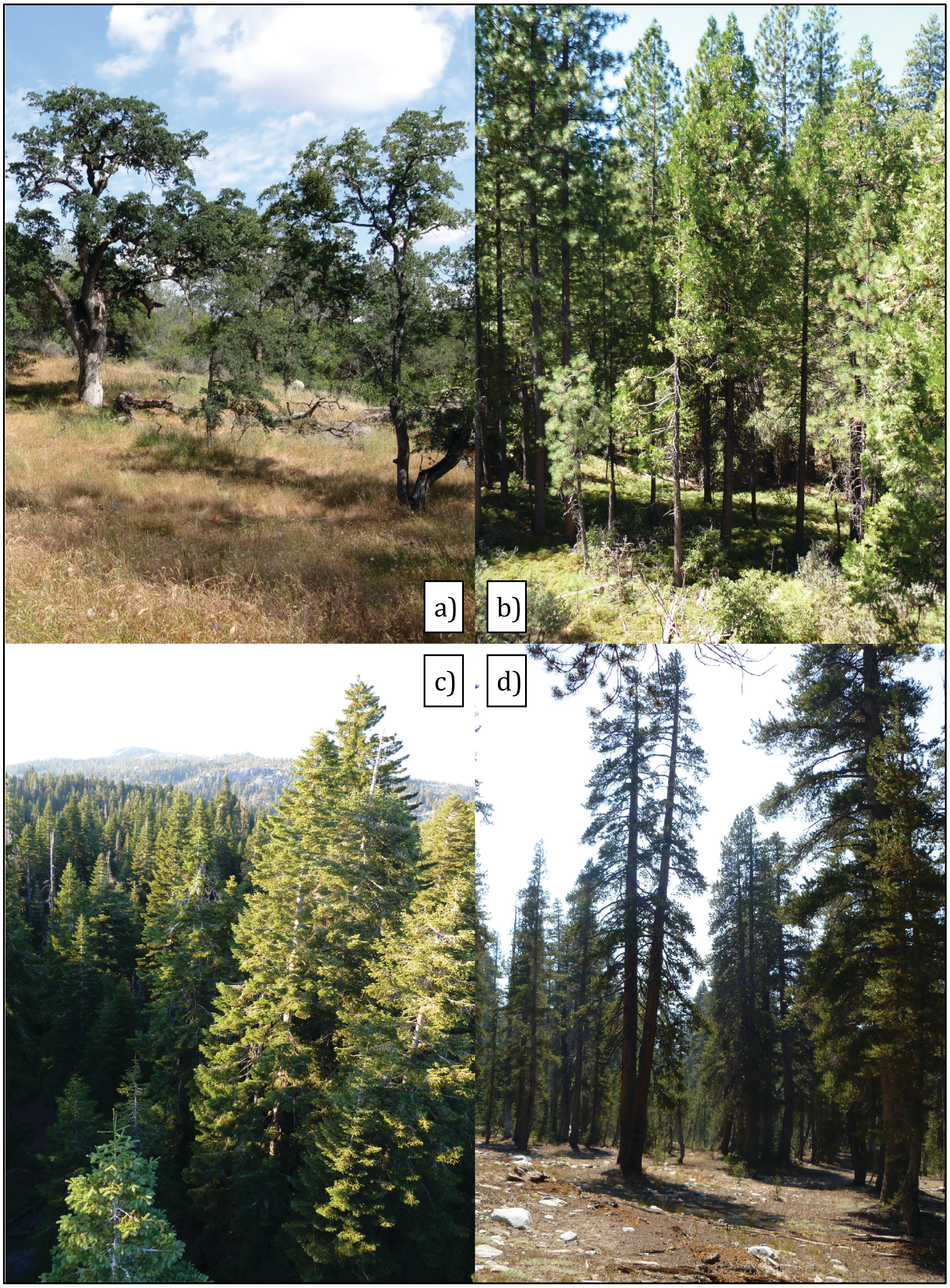

Figure 2.2. Photos of the four sites in summer 2010. a) Oak savannah at 405 m, b) Ponderosa forest at 1165 m, c) Sierra mixed conifer forest at 2015 m, d) Lodgepole forest at 2700 m.

Table 2.1. Site characteristics.

Ecosystem type	Elevation (m)	Latitude (^{0}N)	Longitude (^{0}W)	Tower height (m)	Start of measurements
Oak savannah	405	37.109	-119.731	23	24 Sep 2009
Ponderosa forest	1160	37.031	-119.256	34	22 Jul 2010
Mixed conifer forest	2015	37.067	-119.195	49	4 Sep 2008
Lodgepole forest	2700	37.067	-118.987	34	23 Oct 2009

2.2.2. Site descriptions

Measurements were made at four sites within the Sierra National Forest on the western slope of the Sierra Nevada Mountains in Fresno and Madera Counties, California. The sites were situated at approximately 800 m elevation intervals, spanning 65 km east to west [Figure 2.3, Table 2.1]. Ground-based measurements were focused within a 200 m x 50 m (1 ha) plot at each of the four sites. Plots were oriented along the dominant daytime wind direction at each site.

Table 2.2. Weather means for WY 2009-2012.

	Oak savannah	Ponderosa forest	Mixed conifer forest	Lodgepole forest
Annual temp. (^{0}C)	17.6	13.9	9.0	5.3
Feb mean	9.9	6.1	1.2	-1.6
July mean	28.3	23.4	18.3	14.5
Annual precip. (mm)	557	912	1031	1190
Midday VSD (kPa)	2.0	1.6	1.1	0.8

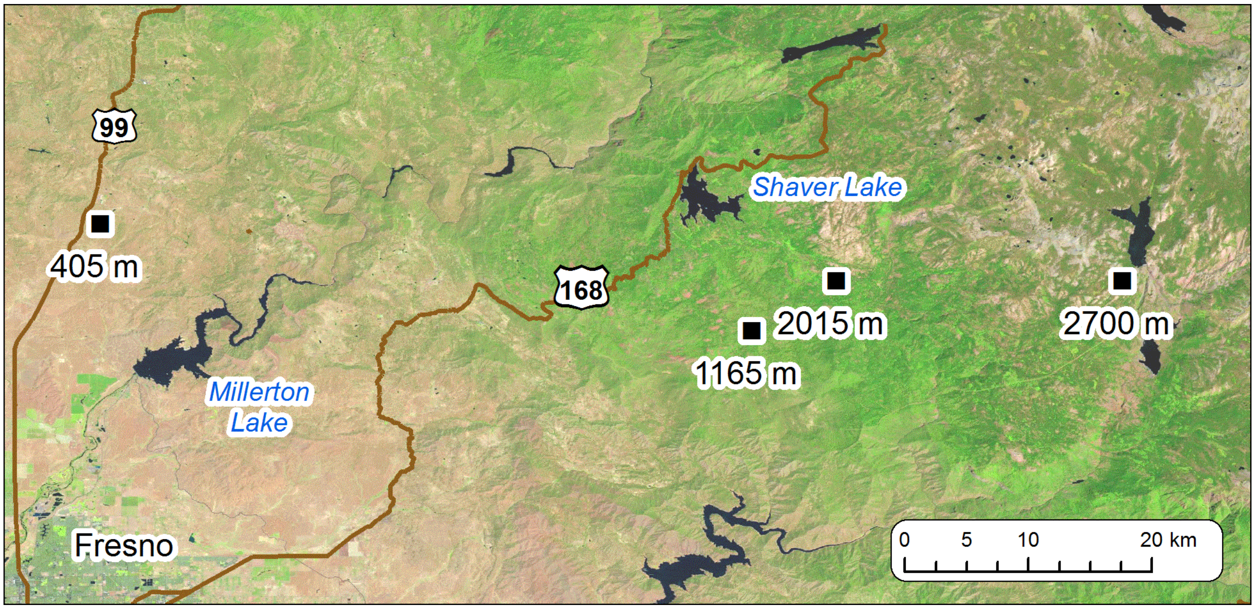

Figure 2.3. Site layout on LANDSAT false color (5-4-3).

The lowest site was oak savannah at 405 m elevation within the San Joaquin Experimental Range. Dominant vegetation was blue oak (*Quercus dumosa*), interior live oak (*Quercus wisleznii*), foothill pine (*Pinus sabiniana*), evergreen shrubs, and annual grasses [

Table 2.3].

The second site was ponderosa forest at 1160 m elevation. Dominant vegetation was ponderosa pine (*Pinus ponderosa*), incense cedar (*Calocedrus decurrens*), canyon live oak (*Quercus chrysolepis*), and a dense understory of evergreen and deciduous subshrubs [

Table 2.3].

The third site was mixed conifer forest at 2015 m elevation in the Kings River Experimental Watershed. Dominant vegetation was white fir (*Abies concolor*), incense cedar, and sugar pine (*Pinus lambertiana*) [

Table 2.3]. Patchy understory included evergreen and deciduous shrubs. The stand was thinned in May 2012 and 5% of the trees within the study plot were harvested.

The fourth site was lodgepole forest at 2700 m elevation. Dominant vegetation was lodgepole pine (*Pinus contorta*) and red fir (*Abies magnifica*) with mostly bare soil and a patchy understory of perennial evergreen herbs [

Table 2.3].

Table 2.3. Biomass in a 1 ha plot around each tower site and date first measured. Top three dominant species' biomasses are also listed, except in the lodgepole forest where only two species were present.

Biomass	tC ha^{-1}	Date
Oak savannah	**18.6**	**26 May 2010**
Quercus wisleznii	8.8	
Quercus dumosa	6.9	
Pinus sabinina	2.9	
Ponderosa forest	**59.9**	**14 Jul 2010**
Pinus ponderosa	34.8	
Calocedrus decurrens	8.4	
Quercus kelloggii	7.7	
Mixed conifer forest	**90.9**	**02 Sep 2009**
Abies concolor	66.7	
Calocedrus decurrens	8.3	
Pinus lambertiana	8.3	
Lodgepole forest	**82.6**	**24 Jun 2010**
Pinus contorta	81.5	
Abies magnifica	1.1	

2.2.3. Meteorology and gas fluxes

Data were collected October 2009 through October 2013, or water years (WYs) 2010 – 2013. Eddy covariance measurements began between September 2008 and July 2010 [Table 2.1]. Ground-based meteorology and eddy covariance measurements at the lodgepole forest ceased when the tower was damaged in May 2012. Tower-based measurements at all other sites continued through the end of WY 2013.

Air temperature and radiation were measured at the tower tops of each site, approximately 5 m above canopy height [Table 2.1]. Air temperature was measured with a Campbell Scientific HMP45C probe (Logan, UT, USA).

Turbulent fluxes of CO_2, H_2O, sensible heat, and latent heat were measured at the tower tops following Goulden et al. [1996]. Eddy covariance fluxes of CO_2 (Net Ecosystem CO_2 Exchange; NEE), water vapor (evapotranspiration; ET), and sensible heat (H) were calculated at half hour intervals from the raw observations of wind velocity made with a sonic anemometer (CSAT-3, Campbell Scientific). CO_2 and water vapor density were measured with a closed-path infrared gas analyzer (LI-7000, LI-COR, Lincoln, NE, USA) [*Goulden et al.*, 2004]. The half-hour fluxes were filtered to remove calm periods (observations with a friction velocity (u*) less than 0.2 m s^{-1}) [*Goulden et al.*, 1996].

The half-hourly gross ecosystem exchange (GEE) was calculated as the difference between observed NEE and respiration determined for 10-day periods. Half-hourly NEE was fit linearly to incoming solar radiation (K) less than 200 W m^{-2} during turbulent periods (u* > 0.2 m s^{-1}). Respiration was determined as the y-intercept of the fit. Half-hourly GEE rates were filled as a function of light and summed to calculate annual gross primary production (GPP).

We used the energy budget closure to confirm that our daytime observations were not systematically less accurate than those reported for lowland, comparatively flat sites. Energy budget closure was determined as the linear regression of net radiation against the sum of latent heat, sensible heat, and soil heat flux. Soil heat flux was calculated from the half-hourly changes in soil heat content determined with thermocouples near the tower at 10, 50, 100, and 200 cm depth. The energy budget linear regression was forced through the origin for half-hourly observations during windy periods (u* > 0.2 m s^{-1}). Energy budget closure was between 77% and 86% at the sites, which is comparable to closure terms reported for eddy covariance at comparatively flat sites [*Turnipseed et al.*, 2002; *Wilson et al.*, 2002; *Foken*, 2008]. Evapotranspiration (ET) and GEE were subsequently corrected for the lack of energy budget closure by dividing fluxes by the energy budget closure term [*Twine et al.*, 2000]. Potential evapotranspiration (PET) was calculated using the Thornthwaite method [*Thornthwaite*, 1948].

Precipitation data came from PRISM [*PRISM Climate Group*, 2013] due to the difficulty of accurately measuring the water content in snowfall. The two lower sites received almost all precipitation as rain, and the tower tipping-bucket rain-gauge data were well correlated with monthly PRISM data for those locations ($R^2 > 0.87$). The two upper sites received over half of their precipitation as snow, and the rain gauge underestimated winter precipitation at these sites.

2.2.4. Ground-based biomass and production measurements

Aboveground woody biomass was assessed by identifying, tagging, and measuring the diameter at breast height (dbh) of all trees > 10 cm dbh within a 200 m x 50 m plot. The plot was oriented around the eddy covariance tower with 150 m of the 200 m leg upwind along the dominant wind direction and 50 m downwind of the tower. Within each plot, 30-50% of trees were randomly selected for dendrometer installation. Dendrometers were measured every two to six months, and increment growth was converted to aboveground stem production using species-specific allometric equations compiled in the Biopak software [*Means et al.*, 1994]. Stem growth for trees without dendrometers was calculated using a linear fit of growth increment to dbh for each species within the plot.

Litter production was measured using forty litter traps equally spaced on a grid within the 1 ha plots. Traps were 43 cm x 53 cm and were collected at the beginning and end of the wet season, in October and May or June. Litter was oven-dried at 65^{0}C for 72 hours and weighed. Aboveground net primary production (ANPP) was calculated as the sum of stem production and leaf litterfall. Grass and herbaceous production were included in ANPP at the oak savannah site; data came from Neil McDougald [SJER USDA *pers. comm*; *George et al.*, 2001].

2.2.5. Fraction of absorbed photosynthetically active radiation (fPAR)

Both fPAR and LAI were taken from the MODIS Terra satellite (Collection 5, accessed 28 January 2014) for the 1 km pixel encompassing the tower location [*Oak Ridge National Laboratory Distributed Active Archive Center (ORNL DAAC)*, 2011]. Eight-day composite observations rated as high quality were obtained for periods with a net carbon uptake (NEE < 0) measured by the tower.

2.3. Results

2.3.1. Climate along the gradient

Growing degree days (GDD) decreased from an average of 3000^0C at the oak savannah to 500^0C at lodgepole forest, using the standard base temperature of 10^0C [Figure 2.4a]. The lapse rate of growing degree days was -1.15^0C m^{-1} ($R^2 > 0.99$). Potential evapotranspiration (PET), calculated using the Thornthwaite method [*Thornthwaite*, 1948], exhibited a similar linear trend with elevation [Figure 2.b], decreasing from an average of 1068 mm yr^{-1} at the oak savannah to 475 mm yr^{-1} at the lodgepole forest. The lapse rate of PET was -0.26 mm m^{-1} ($R^2 > 0.99$).

Precipitation increased with elevation [Figure 2.4c], from 860 mm yr^{-1} at the ponderosa forest to 1040 mm yr^{-1} at the lodgepole forest. The lapse rate above the ponderosa forest was 0.119 mm m^{-1} ($R^2 > 0.99$). Precipitation at the oak savannah was markedly below this trend, at 540 mm yr^{-1}. Interannual variability in precipitation was high, with 2012 and 2013 receiving less than half the precipitation of 2011 [Figure 2.4c].

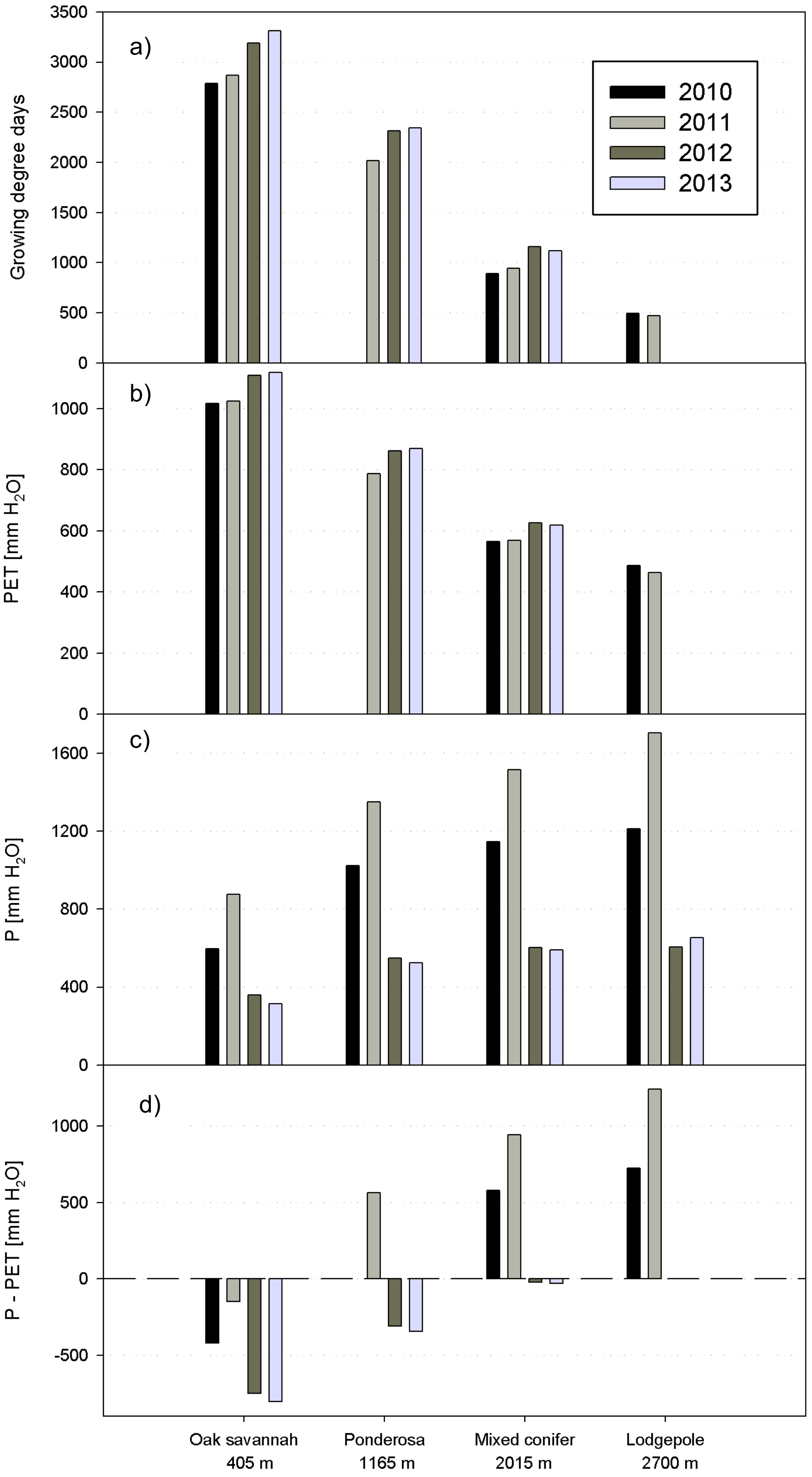

Figure 2.4.Annual water year weather and water balance at the four sites: a) growing degree days, b) potential evapotranspiration, c) precipitation, d) “water balance” = precipitation – PET.

Water balance, defined as PET minus precipitation, increased with elevation [Figure 2.4d]. Water balance increased from a deficit of -532 mm yr^{-1} at the oak savannah to a surplus of 983 mm yr^{-1} at the lodgepole forest. The lapse rate of water balance was 0.636 mm m^{-1} ($R^2 > 0.99$). The mean crossover point, where PET was equal to precipitation, roughly coincided with the lower boundary of the closed-canopy forest.

2.3.2. Biomass and productivity along the gradient

Biomass followed a unimodal curve with increasing elevation [Figure 2.5, 2.6]. Woody biomass was lowest at 18.6 tC ha^{-1} in the oak savannah, peaked at 90.9 tC ha^{-1} in the mixed conifer forest, and decreased slightly to 82.6 tC ha^{-1} in the lodgepole forest [Figure 2.5].

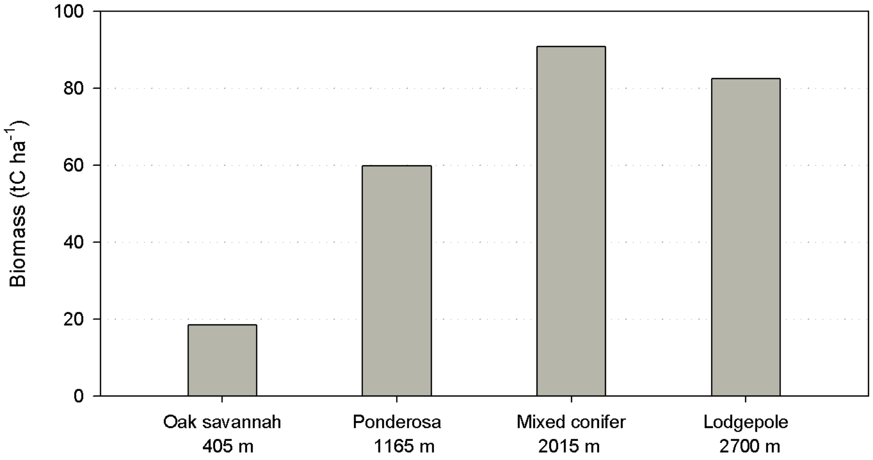

Figure 2.5. Aboveground biomass (tC ha^{-1}).

Gross primary production increased from an average of 7.5 tC ha^{-1} yr^{-1} at the oak savannah, to 17.4 tC ha^{-1} yr^{-1} at the ponderosa forest, before decreasing to 12.9 tC ha^{-1} yr^{-1} at the mixed conifer forest, and 5.8 tC ha^{-1} yr^{-1} at the lodgepole forest [Figure 2.6a]. Gross primary production at the three lowest sites was higher during the wettest years of the study, 2010 and 2011, and reduced during 2012 and 2013.

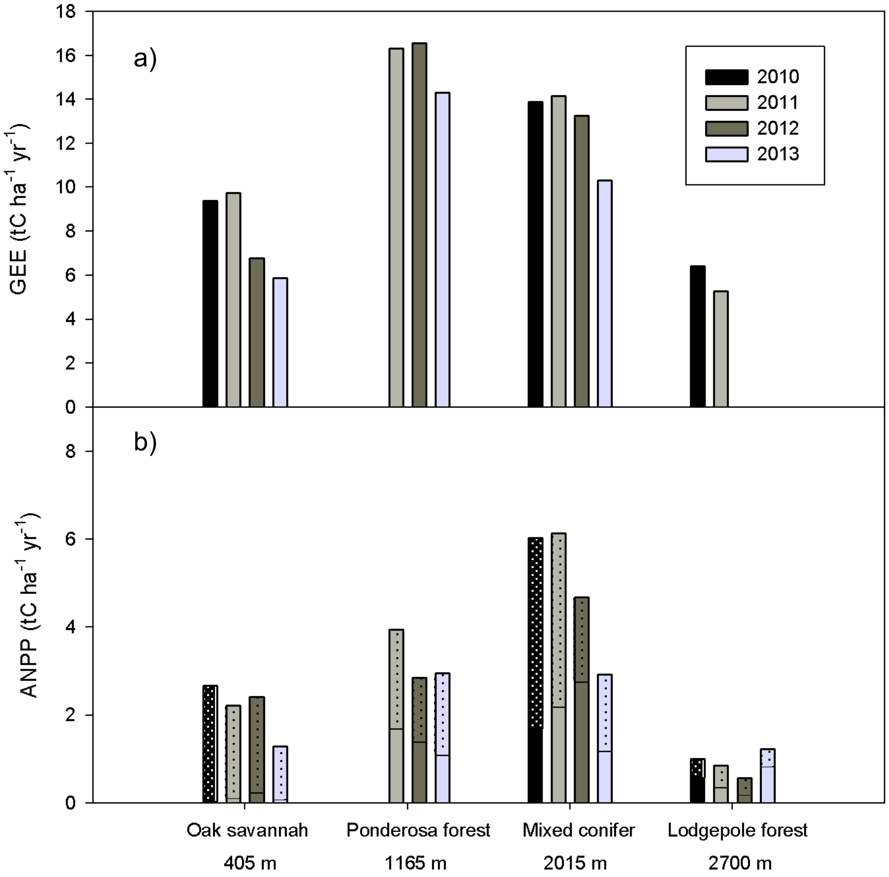

Figure 2.6. Carbon fluxes (tC ha^{-1} yr^{-1}). a) GPP, b) ANPP. Solid fill is stem production, stippled fill is leaf production.

Aboveground net primary production increased with elevation from 2.2 tC ha^{-1} yr^{-1} in the oak savannah to 3.3 tC ha^{-1} yr^{-1} in the ponderosa forest, and 4.9 tC ha^{-1} yr^{-1} in the mixed conifer forest. ANPP was markedly reduced, at 0.9 tC ha^{-1} yr^{-1}, in the lodgepole forest [Figure 2.6b].

Consistent with interannual trends in GPP, ANPP was higher in 2010 and 2011 at the three lowest sites than in 2012 and 2013.

2.3.3. Limitations on primary production and biomass

Gross primary production can be described as the product of growing season length and the daily rate of CO_2 assimilation during the growing season. Growing season length was calculated as the period when 24-hour sums of NEE indicated a net ecosystem uptake. Growing season length followed trends that were similar to annual production, with a nearly symmetric unimodal curve peaking at mid-elevations [Figure 2.7a]. The growing season averaged 180 days at the oak savannah, and 314 days at the ponderosa forest, 328 days at the mixed conifer, and 185 days at the lodgepole sites.

Daily GEE was remarkably similar across sites [Figure 2.7b]. The highest GEE of 46.8 kgC ha^{-1} day^{-1} was observed at the ponderosa forest, and the lowest GEE of 31.4 kgC ha^{-1} day^{-1} at the lodgepole forest. As with GPP and ANPP, GEE rates were higher in 2010-11 at the lowest three sites.

Maximum GEE is limited in part by an ecosystem's photosynthetic capacity. The average fraction of photosynthetically active radiation (fPAR) determined by MODIS during the growing season closely tracked the inter-site and interannual trends in GEE rates ($R^2 = 0.63$, $n = 13$). Maximum growing-season fPAR was 0.73 at the ponderosa forest and minimum growing-season fPAR was 0.32 at the lodgepole forest. Interannual variability in mean fPAR was less than 15% at all sites.

2.3.4. Carbon allocation and turnover

Aboveground carbon use efficiency (ACUE) was calculated as ANPP divided by GPP. Aboveground carbon use efficiency was generally consistent except for a possible decrease at the highest site [Figure 2.Figure 2.8]. Mean annual ACUE was highest at 0.38 at the mixed conifer forest, and lowest at 0.16 at the lodgepole forest. At the lower three sites, ACUE varied by 33-50% of the mean interannually.

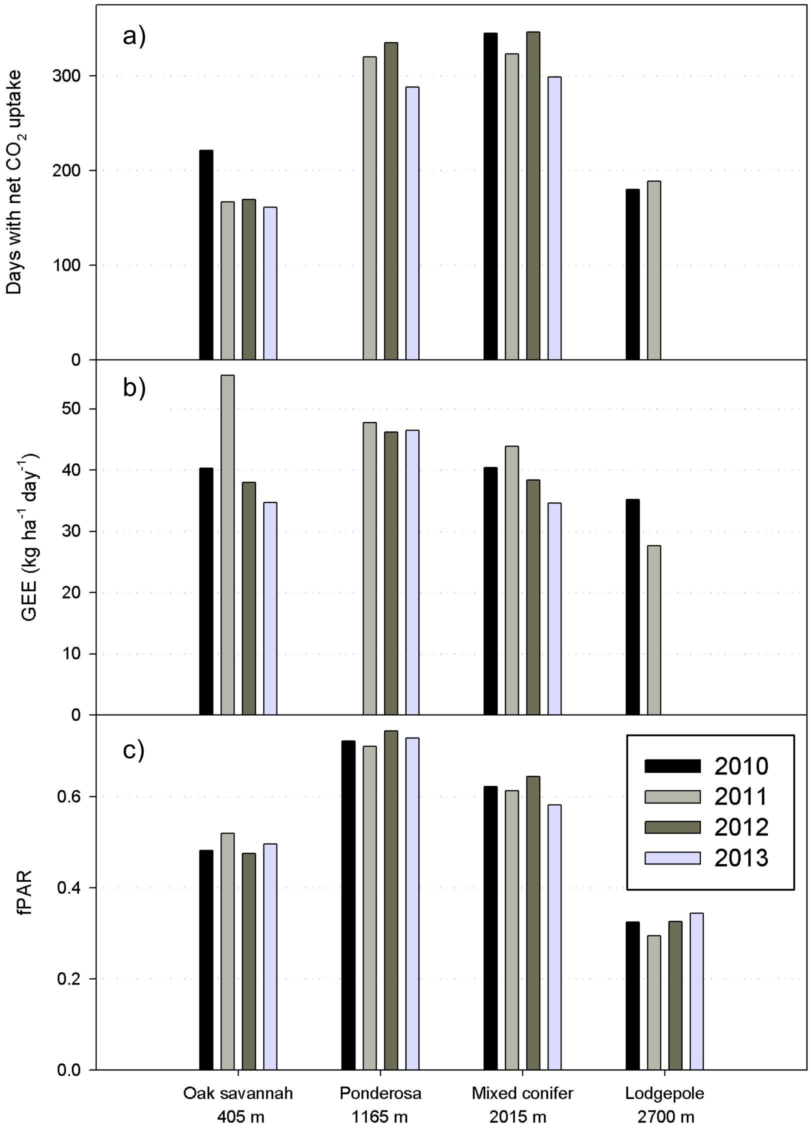

Figure 2.7. Growing season properties. a) growing season length, b) mean daily growing season GEE, c) growing season fPAR.

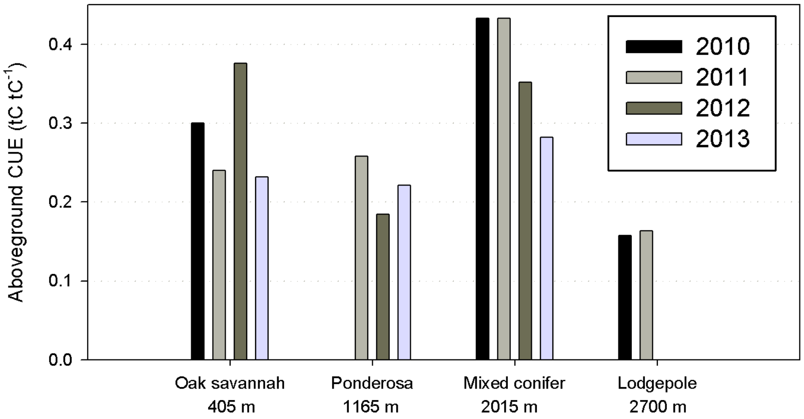

Figure 2.8. Aboveground carbon use efficiency.

Allocation of GPP to tree stems and leaves also exhibits unimodal trends with elevation peaking at the mixed conifer forest [Figures 2.6b; 2.9a, b]. Woody stem allocation ranged from 15% at the mixed conifer forest to 1.6% at the oak savannah [Figures 2.6b; 2.9a]. Leaf production is increasingly dominated by trees, particularly conifers, with increasing elevation, with conifers accounting for 100% of litterfall at the lodgepole forest [Figure 2.Figure 2.9c]. Allocation of GPP to tree leaves followed the same trend with elevation. Tree leaf allocation was a minimum of 6.9% at the lodgepole forest, a maximum of 16% at the mixed conifer forest, declining to 11% at the ponderosa forest, and declining further to 7.3% at the oak savannah (data not shown). Including annual production in leaf allocation produces a less clear trend with elevation [Figure 2.9b]. Over 72% of aboveground primary production in the oak savannah goes to grasses and forbs [Figure 2.9c].

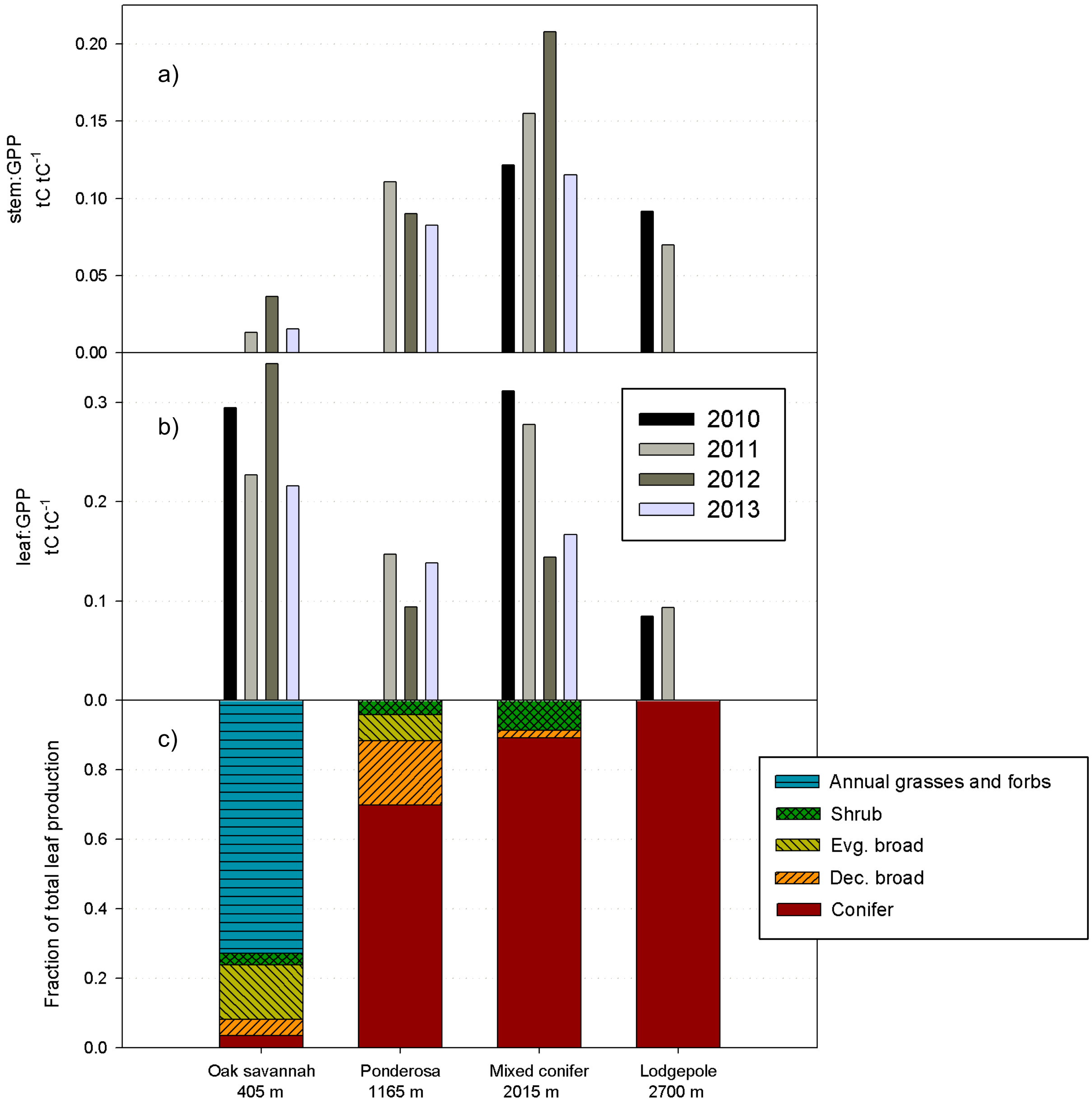

Figure 2.9. Allocation of production. a) stem:GPP, b) leaf:GPP, c) litterfall plant functional type.

Biomass turnover was calculated as woody turnover time (τ_w, Eq. 2.1). Woody turnover time was U-shaped with elevation [Figure 2.10].

Equation 2.1)
$$\tau_w = \frac{aboveground\ biomass}{woody\ stem\ production}$$

Woody turnover times were longest at the oak savannah and lodgepole forest, around 160 years. Woody turnover times were shortest at the mid-elevation ponderosa and mixed conifer forests, around 50 years. Trees at the oak and lodgepole sites were slow growing and long-lived compared to the mid-elevation sites.

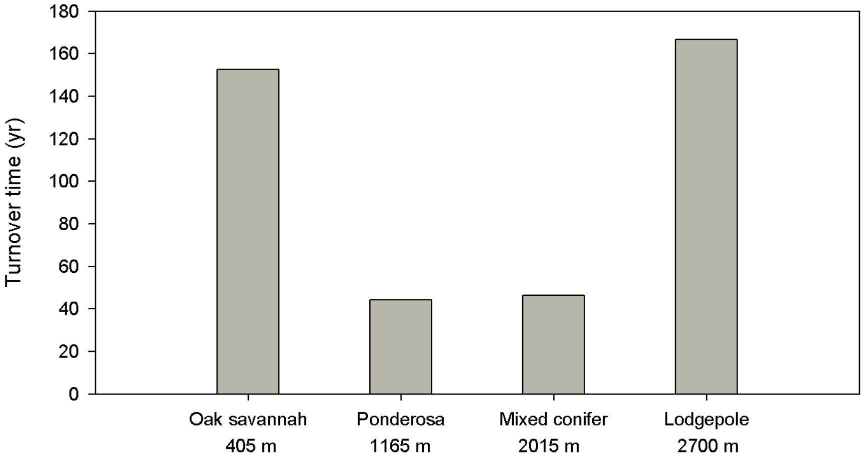

Figure 2.10. Aboveground woody carbon turnover times, τ_w.

2.3.5. Quantifying the diagnostic framework

We used our observations to quantify the parameters of the diagnostic framework in Figure 2.1. Fluxes and pools were each measured independently. Two controls on fluxes, growing season length and daily gross CO_2 uptake, were also measured independently. The remaining three controls on fluxes, aboveground CUE, allocation of ANPP to wood, and carbon turnover time, were calculated using observed fluxes. Control values are summarized in Table 2.4.

Table 2.4. Summary of control values in the diagnostic framework [Figure 2.1].

	Growing season days yr^{-1}	Daily gross CO_2 uptake kg day^{-1}	Aboveground CUE % yr^{-1}	Allocation of ANPP to wood % yr^{-1}	Carbon turnover time yr
Oak savannah	180	31.6	28.7%	5.9%	152
Ponderosa forest	314	44.5	22.1%	43.1%	44
Mixed conifer forest	328	38.4	37.5%	40.9%	46
Lodgepole forest	185	31.6	16.0%	42.8%	167

Carbon fluxes were observed directly [Table 2.5]. Because of the small number of trees and short observation period relative to tree lifespans, observed tree mortality did not reflect long-term average of tree mortality in this forest. Tree mortality was not observed at the oak savannah, likely due to the very small number of long-lived trees.

Table 2.5. Summary of flux values in the diagnostic framework [Figure 2.1].

	Gross primary production tC yr^{-1}	Aboveground NPP tC yr^{-1}	Gross wood production tC yr^{-1}	Woody mortality[1] % yr^{-1}
Oak savannah	7.6	2.2	0.1	0.0%
Ponderosa forest	14.7	3.3	1.4	0.0%
Mixed conifer forest	12.9	4.9	2.0	1.1%
Lodgepole forest	5.8	0.9	0.5	1.0%

---

[1] Woody mortality was calculated as the biomass of trees that died during the course of the study.

2.4. Discussion

2.4.1. How and why do GPP and NPP vary with climate?

Gross primary production is determined by growing season length and maximum photosynthetic rate. Growing season length is typically constrained by cold temperatures in winter, and water stress in summer. The oak savannah had a growing season of 180 days that was limited by high temperatures and summer drought. Conversely, the lodgepole forest had a growing season of 185 days that was constrained by winter dormancy with cold conditions. The growing season was 314 days at the ponderosa forest and 328 days at the mixed conifer forest. These two sites had no prolonged cold- or drought-induced dormant periods, and photosynthesis was limited only intermittently by cloudy conditions during winter storms.

Ecosystem leaf area index (LAI) typically limits maximum GEE during the growing season. The fraction of absorbed photosynthetically active radiation (fPAR) is closely related to LAI and thus provides an indicator of ecosystem photosynthetic capacity [*Field et al.*, 1995; *Running et al.*, 2000]. The elevational trend of fPAR during the growing season followed the same pattern as mean daily GEE ($R^2 > 0.71$). Growing season fPAR and mean daily GEE were highest at 1160 m and lowest at the lodgepole forest. Daily GEE varied by just 16% between sites. Daily GEE at the three warmest sites was higher in WY 2011, the wettest year of the study. At the lodgepole forest, daily GEE was lower in WY 2011, associated with an abnormally heavy snowpack.

Gross primary production, daily GEE, and fPAR peaked at the ponderosa forest, but ANPP peaked at the mixed conifer forest [Figure 2.6, 2.8]. These mid-elevation sites were the most similar of the four sites investigated; the two sites shared some common species and congeners, albeit in different proportions.

We expect that the difference between sites in aboveground carbon use efficiency is due to differences in respiration rates and aboveground/belowground allocation of carbon. Greater water deficit at the ponderosa forest [Figure 2.5d] could drive trees to allocate more carbon to roots. A similar ponderosa forest in Oregon allocated 61% of GPP to root production, attributed to water limitation [*Law et al.*, 2008]. Also supporting this hypothesis is sharply declining ACUE in the mixed conifer forest in dry years.

Higher temperature, and thus a higher maintenance respiration rate, is another possible cause of reduced ACUE at the ponderosa forest. Ryan and Waring [1992] found that stand age was not a factor in ACUE, but temperature drove important differences in respiration rates and thus net carbon assimilation. Ryan et al. [1995] found that ACUE decreased with increasing temperature across four types of conifer forest. This is consistent with our findings for the two mid-elevation sites: ACUE decreases and production increases with increasing temperature between these sites. Carbon allocation rather than increasing respiration is the primary control on ACUE at the oak savannah and lodgepole sites.

Standing biomass is controlled by the balance of gross wood production and mortality. Whether the GPP of an ecosystem translates into woody biomass/long-term carbon storage depends on the carbon use efficiency of the system. Aboveground carbon use efficiency peaked at the mixed conifer forest, where ANPP, growing season length, and biomass also peaked [Figure 2.5].

The oak savannah exhibited moderate ACUE and higher interannual variability in ACUE than the other sites. Gross primary production at this site is also moderate, limited by a short growing season truncated by summer heat and drought. Allocation to woody biomass is the lowest of all the sites; ANPP at this site is dominated by grass and forb production. The combination of a short growing season and low allocation to woody biomass results in the lowest standing biomass of the four sites.

2.4.2. How and why does biomass vary with climate?

Biomass followed a unimodal curve along a gradient of increasing precipitation and decreasing temperature, and peaked at the mixed conifer forest. The lodgepole site exhibited the lowest ACUE of all the sites despite supporting the second-highest biomass. Gross primary production, ANPP, daily GEE, and FPAR were all lowest at this site compared to the other three sites. Gross primary production at the lodgepole forest is limited by low GEE and a short summer growing season. This site is slow-growing with a limited capacity for production based on fPAR. The large standing biomass is due to the slow rate of carbon turnover as opposed to a fast rate of carbon accumulation.

The elevational trend of allocation of GPP to stems closely follows the elevational trend of biomass. Stem allocation peaks at the mixed conifer forest, is similar between the ponderosa forest and lodgepole forest, and is an order of magnitude less at the oak savannah. Stem wood is the primary component of aboveground biomass, and thus it is unsurprising that aboveground allocation of GPP correlates with biomass. There is a subtle but important difference between the ponderosa forest and the lodgepole forest. The lodgepole forest has 37% greater biomass than the ponderosa forest, but stem allocation of GPP is nearly the same. This difference is consistent with our observations of larger, slower-growing trees at the lodgepole compared to the ponderosa forest.

Water balance (precipitation minus PET) was negative every year during the study period in the oak savannah. Water balance fluctuated between negative and positive interannually in the ponderosa forest, and was always positive at the mixed conifer site. The ponderosa forest therefore experienced a much greater interannual variability in water stress than the mixed conifer forest. The ponderosa site was just above the lower boundary of the closed canopy forest, and likely at the physiological limit of closed canopy conifer forest. This suggests the boundary between chaparral and closed-canopy forest, a sharp boundary between low and high biomass vegetation, is coincident with the elevation where mean annual water balance flips from deficit to surplus.

2.4.3. Implications

The climate gradient on the slope of the western Sierra Nevada produces non-linear trends in gross production, net production, mortality, and biomass along the gradient. Below ~1100 m, summer drought truncates ecosystem production, and above ~2100 m, winter cold limits ecosystem production. Ecosystem production and mortality rates together determine the amount of standing biomass, which peaks in the mild mid-elevations. Our framework-based biomass estimation shows the strongest climate-related control on biomass is growing season length and carbon turnover time. Daily growing season CO_2 uptake, ACUE, and woody allocation are only weakly correlated with temperature and precipitation. Our diagnostic framework of biomass suggests that climate changes such as warming and drought would affect ecosystems differently across the gradient.

Our predictions are consistent with recent findings in Southern California. The mountains of Southern California have nearly identical tree species to the mid-elevation conifer forest on our gradient, yet biomass in the conifer forest of Southern California mountains averaged around 57 tC ha^{-1} [*Walker et al.*, 2004] while the conifer forest along our gradient has an average biomass around 71 tC ha^{-1}. The diagnostic framework is consistent with higher biomass in the central Sierra comparable to the warmer, drier mountains of Southern California. Fellows and Goulden

[2012] found that lower elevation ranges of the conifer forest and individual species experienced significantly greater mortality with drought and warming than upper elevations, consistent with our prediction of greatest biomass loss at the lowest extent of the conifer forest under both the warming and drying scenarios.

Warming increases carbon turnover times and photosynthetic rates. Warming also truncates the growing season for drought-stressed systems and extends the growing season for cold-limited systems. With warming, the oak woodland and mixed conifer forests might be the least impacted. Biomass in the oak savannah has been limited by heat and drought stress. Biomass in the few oak and pine trees might die back with warming, and production would likely continue to be dominated by annual grasses and forbs.

Each of the three conifer forest sites would respond differently to increased warming and drought. The ponderosa forest has survived at its geographic and physiological limits. With warming, mean annual water deficit would become more consistently negative. Episodic mortality would increase and production would decrease. The mixed conifer forest would experience faster carbon turnover with warming and a decrease in annual water balance. Either of these changes could promote increased episodic mortality and decrease standing biomass. The lodgepole forest would experience an increase in growing season and production rates with warming, and could become a larger-statured, more diverse forest.

Increased drought would result in widespread reduction in biomass at all but the highest elevations. Drought stress already limits photosynthesis rates and growing season length at the oak savannah. Increased water deficit could push the lower elevation boundary of the forest above the existing ponderosa site, and the mixed conifer forest could experience late summer drought stress. The lodgepole forest could increase production with drought, as its growing season was limited by winter cold [*Trujillo-Gomez et al.*, 2012]. This forest could show an increase in biomass with drought.

Chapter 3. A montane Mediterranean climate supports year round growth and high biomass

Abstract

The most massive trees in the world are found in mid-elevation mixed conifer forest in the central Sierra Nevada Mountains in California. Mortality in this forest has been increasing and has been associated with recent drought and warming, but direct measurements of Sierra forest physiology have been lacking. We wish to understand the climatic limitations on forest physiology in this Mediterranean snow-dominated system for better predictions of forest responses to future climate scenarios. We used eddy covariance and direct aboveground primary productivity measurements to understand how winter cold and summer drought limit growth and annual production within this forest type at a mid-elevation site in the Kings River Experimental Watershed in the Southern Sierra Nevada. We found that net production in this forest was limited neither by winter cold nor summer drought: tree growth continued year-round and net photosynthetic uptake continued during sunny periods at an air temperature below 0^{o}C, and throughout the summer dry period. The year-round growing season allowed the forest to take advantage of winter precipitation and warm summer weather, and promoted the existence of a forest with biomass and productivity similar to tropical rainforest.

3.1. Introduction

The mid elevations of California's Sierra Nevada range pose a bioclimatic paradox. The 1500 – 2500 m elevation band is a Mediterranean climate in the rain-snow transition zone, with near-freezing winters and long, rain-free summers. The asynchrony between winter moisture availability and summer warmth suggests a brief growing season in the late spring and early summer [*Urban et al.*, 2000], yet this is a large-statured forest and the endemic range of the most massive trees in the world, the giant sequoia (*Sequoiadendron giganteum* (LINDL.) J. BUCHH.). Bioclimatic correlations incorrectly predict steppe, savannah, or deciduous forest for the climate envelope of the mid-montane Sierra, and consequently underpredict biomass and productivity [e.g. *Rosenzweig*, 1968; *Lieth*, 1975; *Potter et al.*, 1993; *Urban et al.*, 2000]]. How Sierra mixed conifer forest supports biomass comparable to tropical rainforests in this seemingly harsh environment remains an unsolved problem. The question of how the high-biomass forest survives in winter cold and summer dry montane Mediterranean climate has been explored in the literature. Studies thus far have suggested that late-summer drought stress and winter cold limit production in Sierra mid-elevation mixed conifer forest [*Royce and Barbour*, 2001; *Stephenson*, 1998; *Urban et al.*, 2000]. Field observations of climate controls on Sierra Nevada growing season, production, and water use remain scant [*Araujo and Petersen*, 2012].

The forest of the Sierra Nevada is a major component of California's carbon and water budgets. The Sierra Nevada is estimated to have 69 tC ha^{-1}, or about 20% of California's standing biomass, but is also estimated to be losing carbon at the rate of 0.4 tC ha^{-1} yr^{-1} [*Potter*, 2010]. The Sierra Nevada is also critical to California's water supply, providing a natural seasonal reservoir of water in its winter snowpack and over 60% of the state's water consumption [*California Department of Water Resources*, 2005; *Bales et al.*, 2011a].

Recent observations suggest that the Sierra mid montane forest is nearing its physiological limits. Forest mortality has been increasing in recent years, which has been attributed to increasing drought stress with climate warming [*Van Mantgem and Stephenson*, 2007]. However, the specific climatic thresholds for forest mortality in the Sierra Nevada are unknown. California has experienced recent warming and increased precipitation variability, and these trends are expected to continue [*Cayan*, 1996; *LaDochy et al.*, 2007; *Cayan et al.*, 2008; *Abatzoglou et al.*, 2009]. To understand the Sierra forest's vulnerability to climate change and accurately predict its future, we need a better understanding of the forest's physiological responses to meteorological conditions and accurate predictions of the future of California's water and carbon resources with climate change [*Dettinger et al.*, 2004; *Barnett et al.*, 2005; *Loarie et al.*, 2008; *Flint and Flint*, 2012].

We made direct measurements of ecosystem and meteorological properties to better understand the relationships between weather, biomass, productivity, and water use. Our research focuses on three questions: 1) To what extent does winter cold limit gross primary production, net primary production, and evapotranspiration? 2) To what extent does the combination of dry soils and warm daytime temperatures in summer limit gross primary production, net primary production, and evapotranspiration? 3) How would a warmer or drier climate affect forest production, water use, and vulnerability to mortality?

3.2. Methods

3.2.1. Site description

Measurements were made in the Kings River Experimental Watershed [*Eagan et al.*, 2007] at an elevation of 2015 m in the central Sierra Nevada Mountains (37.0675^{0}N, -119.1951^{0}W).

Measurements were made during water year (WY) 2009 through most of WY 2012 (September 1, 2008 – May 31, 2012). We defined autumn as September – November, winter as December – February, spring as March – May, and summer as June – August.

The study area was in the Sierra National Forest, about 10 km southeast of Shaver Lake and 0.5 km southwest of the end of Forest Service Road 10S10. Access was by vehicle in summer and foot in winter. Micrometeorological measurements were made on a 55 m tall eddy covariance tower. Intensive ground-based measurements were focused in a 200 m by 50 m (1 ha) plot, which extended 150 m in the mean upwind direction and 50 m downwind. The broad relief was a ~10° downhill slope in the southwest direction, with a 2° slope in the study plot [Figure 3.1].

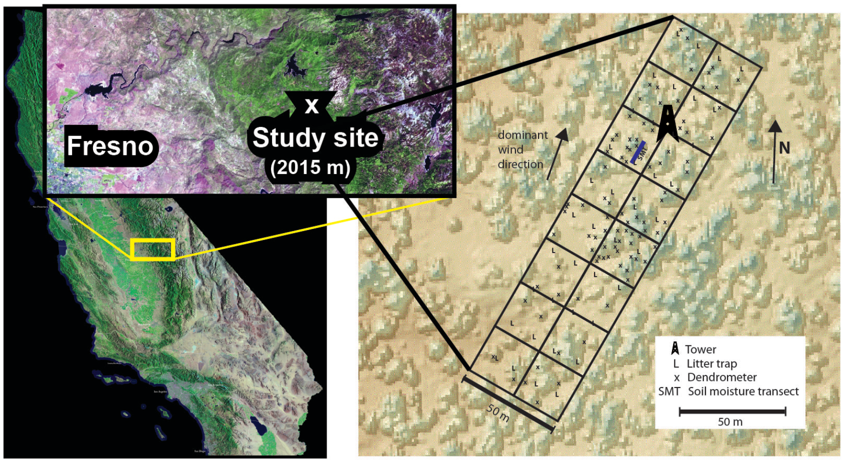

Figure 3.1. Plot layout and location within California. Inset image is LANDSAT ETM+ bands 5-4-3 (August 2002). Right image is a NSF NCALM LiDAR image (July 2010) with hillslope and tree shading.

The climate at the site was Mediterranean, with warm dry summers and cool wet winters. Most precipitation fell between October and April, and about 70% fell as snow [*Bales et al.*, 2011b]. Soils were in the Gerle-Cagwin families association [*USDA*, 2009].

The site was mixed conifer forest dominated by Sierra white fir (*Abies concolor* (GORDON & GLEND.) LINDL. EX HILDEBR.) with subdominant California incense cedar (*Calocedrus decurrens* (TORREY) FLORIN), Jeffrey pine (*Pinus jeffreyi* (GREV. & BALF.)), sugar pine (*Pinus lambertiana* (DOUGLAS)), and black oak (*Quercus kelloggii* (NEWB.)) [Figure 3.2]. The forest canopy was patchy, with closed stands of mature white fir and pine and open stands of yellow pine, oak, and shrubs on rockier locations. The understory in areas of open tree canopy consisted of mostly whitethorn (*Ceanothus cordulatus* (KELLOGG)) and greenleaf manzanita (*Arctostaphylos patula* (GREENE)). A nearby grove of giant sequoia grew at the same elevation 10 km to the southeast (the McKinley Grove).

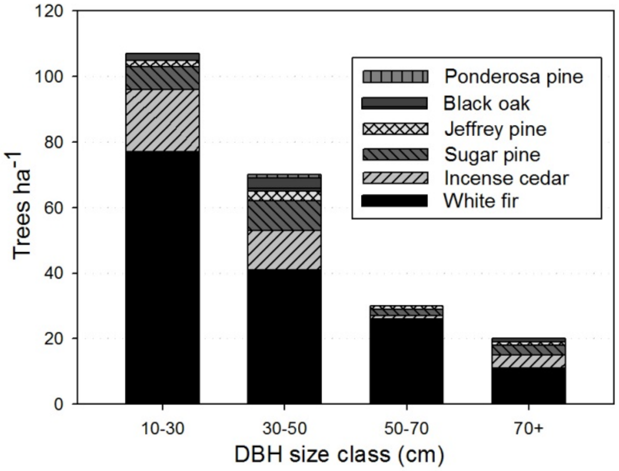

Figure 3.2. Stand demographics in September 2008, including all trees with dbh > 10 cm within the 1 ha plot.

3.2.2. Physical environment measurements

We used a multiscale approach to measure the effects of meteorology on forest physiology and production in Sierra mixed conifer forest [Figure 3.1]. We used a combination of techniques, including half-hourly measurements of weather and stand-level gas and energy exchange, as well as monthly-to-annual measurements of tree growth, litterfall, and mortality. This study focused on a 1 ha study plot in the footprint of an eddy covariance tower.

Radiation and other meteorological conditions were measured at the top the eddy covariance tower and averaged at half-hour intervals. Air temperature was measured at 2, 10, 25, and 55 m heights using aspirated shields and Campbell Scientific [CS; Logan, UT] T-107 thermistors.

Precipitation was measured using a CS TE-525 tipping-bucket rain gauge at the tower, and gaps in the precipitation record were filled with data from the National Atmospheric Deposition Program station CA29 - Kings River Experimental Watershed, 2 km from the tower [*National Atmospheric Deposition Program*, 2013]. Tower and NADP precipitation data were well-correlated during overlapping periods ($R^2 > 0.8$). Potential evapotranspiration (PET) was calculated using the Thornthwaite method [*Thornthwaite*, 1948].

Soil volumetric water content (VWC) was measured with Campbell Scientific CS-616 water content reflectometers. Four probes inserted vertically into the surface of the mineral soil along a 30 m transect.

3.2.3. Turbulent fluxes

Eddy covariance fluxes of CO_2 (Net Ecosystem CO_2 Exchange; NEE), water vapor (evapotranspiration; ET), and sensible heat (H) were calculated at half hour intervals. Wind velocity was measured with a CS CSAT3 sonic anemometer. CO_2 and water vapor density were measured with a LI7000 closed-path Infrared Gas Analyzer (LiCor; Lincoln NE) [*Goulden et al.*, 1996, 2004]. The half-hour fluxes were filtered to remove calm periods (observations with a friction velocity (u*) less than 0.2 m s^{-1}) [*Goulden et al.*, 1996]. The half-hourly gross ecosystem exchange (GEE) was calculated as the difference between observed NEE and the respiration determined for 10-day periods. Respiration was calculated as the y-intercept of a linear fit to the half hour NEEs during windy periods with incoming solar radiation (K) less than 200 W m^{-2}.

We used the energy budget closure to confirm that our daytime observations were not systematically less accurate than those reported for lowland, comparatively flat sites. Energy budget closure was determined as the linear regression of net radiation against the sum of latent heat, sensible heat, and soil heat flux. Soil heat flux was calculated from the half-hourly changes in soil heat content determined with thermocouples near the tower at 10, 50, 100, and 200 cm depth. The energy budget linear regression was forced through the origin for half-hourly observations during windy periods ($u^* > 0.2$ m s^{-1}). Energy budget closure was 86%, which is comparable to that reported for eddy covariance at comparatively flat sites [*Turnipseed et al.*, 2002; *Wilson et al.*, 2002; *Foken*, 2008]. Evapotranspiration (ET) and GEE were subsequently corrected for the lack of energy budget closure by dividing all fluxes by 0.86 [*Twine et al.*, 2000].

Seasonal and annual totals of ET and GEE were calculated by summing after filling intervals with missing, calm, or otherwise unsuitable observations [*Goulden et al.*, 1996; *Moffat et al.*, 2007]. Missing ET observations were filled as a linear function of K, and missing GEE as a nonlinear function of K. Missing observations were more common in winter when snow and low solar angles depleted battery charge. Usable eddy covariance observations were available for 88.5% of the daylight periods in spring and summer, and 60.1% of the daylight periods in autumn and winter. The uncertainty associated with filling missing observations as a function of environmental conditions is typically minor [*Goulden et al.*, 1996; *Moffat et al.*, 2007].

3.2.4. Biomass and production measurements

Aboveground biomass and species composition were measured in September 2009 by identifying, tagging, and measuring the diameter at breast height (dbh) of all trees with dbh greater than 10 cm [Figure 3.2]. Species-specific allometric equations were used to covert dbh to aboveground stem biomass [*Means et al.*, 1994]. Aboveground stem increment was measured using dendrometer bands. Ninety-eight of the 229 trees in the plot (dbh > 10 cm) were fitted with dendrometer bands [*Hall*, 1944; *Keeland and Young*, 2007], which were measured every 4 – 12 weeks during the study. We estimated stem increments for trees without dendrometers by regressing measured growth increments to diameter for each species.

Litter production was measured using forty 26 cm x 56 cm plastic trays arrayed in a grid within the plot. The trays were collected once during the growing season, once before snowfall, and immediately after snowmelt. Litter was dried at 65^{0}C and weighed to calculate litterfall biomass by ground area.

3.3. Results

3.3.1. Meteorology

The meteorological conditions observed were typical of a mid-elevation, snow-dominated Mediterranean climate. Precipitation averaged 1102 mm yr^{-1} during the study period, with 90% falling between October 1 and April 15 [Table 3.1]. Precipitation generally arrived in multi-day winter storms, and about 70% fell as snow during WYs 2008 and 2009 [*Bales et al.*, 2011b]. A snowpack persisted through most of the winter. [Figure 3.3; *Stephenson*, 1988]. Mean annual temperature measured at the tower top during WY 2009 – 2012 was 9.0^{0}C. Summer mean high temperature (JJA) was 18.4^{0}C and mean low was 14.1^{0}C. Winter mean high temperature (JFM) was 5.1^{0}C and mean low was 0.4^{0}C. Summer midday temperatures were 2.6^{0}C higher at 2 m height than the tower top, and night-time temperatures were 2.1^{0}C colder at 2 m than at the tower top [Figure 3.4a]. Winter midday temperatures were not significantly different between 2 and 55 m heights, while night-time temperatures were 2.0^{0}C colder at 2 m than 55 m [Figure 3.4b].

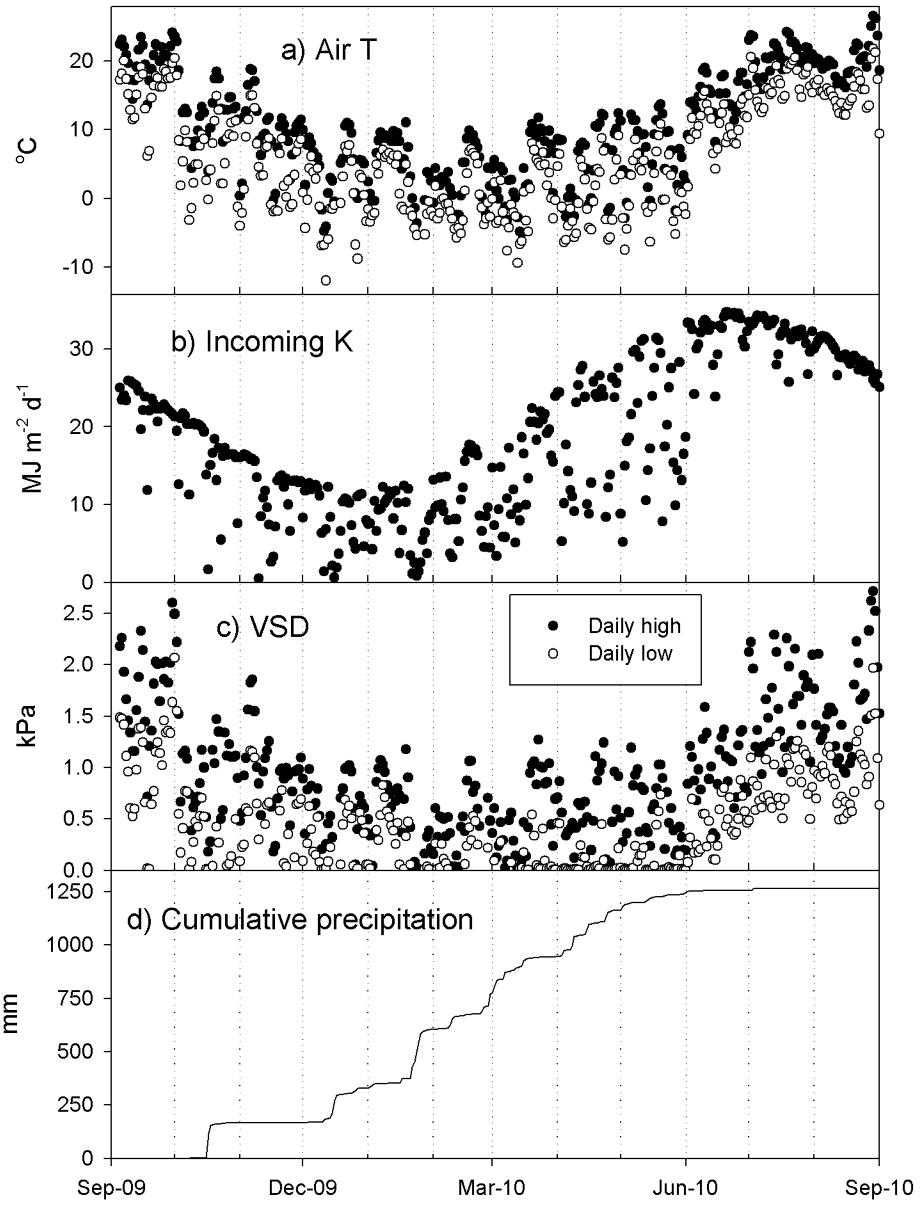

Figure 3.3. Weather in water year 2010. a) Daily high (close circles) and low (open circles) air temperatures measured at the tower top (^{0}C), b) daily total incoming solar radiation (MJ m-2 d-1), c) daily high and low vapor saturation deficit (kPa), and d) cumulative precipitation (mm).

Table 3.1. Weather at the tower site measured during water years 2008-12 (Sept. 1, 2007 – Aug. 31, 2012).

Annual air T (°C)				Mean annual precipitation	Mean annual contiguous period with precip < 1 mm/day
2 m		55 m			
Max	Min	Max	Min		
11.7	7.1	10.5	9.2	1102 mm	138 days

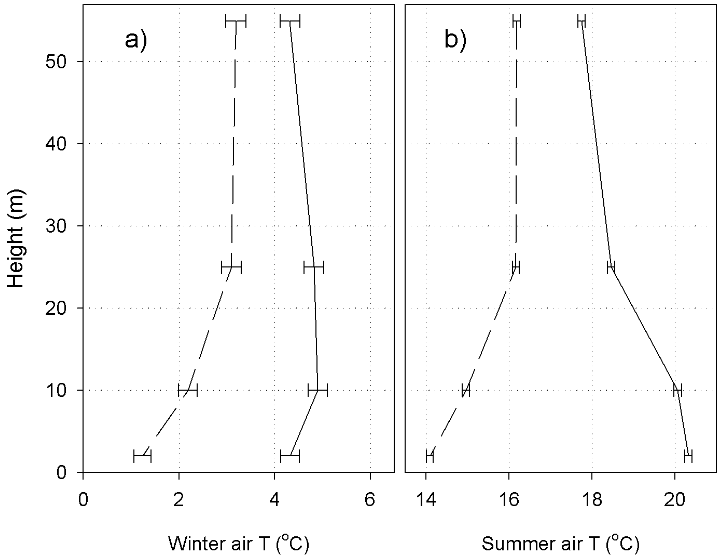

Figure 3.4. Air temperature at 2 m, 10 m, 25 m, and 55 m above ground level during the day (solid lines) and at night (dashed lines) during a) winter (DJF) and b) summer (JJA). Error bars are standard errors of the means.

3.3.2. Tree biomass and production

Aboveground tree stem biomass was 91 tC ha^{-1} in September 2009. Stem growth continued year round, with about 40% of annual growth occurring in the summer and the remaining growth spread evenly through the rest of the year. Gross woody growth averaged 2.1 tC yr^{-1}, and was 2.0 tC yr^{-1} after accounting for mortality. Annual stem production varied by less than 0.15 tC ha^{-1} from year to year. Most leaf mass fell in late summer and early autumn, and consisted primarily of several-year-old senescing conifer needles. Annual litterfall was 4.7 tC ha^{-1} yr^{-1}, which was about twice stem growth. Aboveground net production averaged 6.7 tC yr^{-1} [Figure 3.5c].

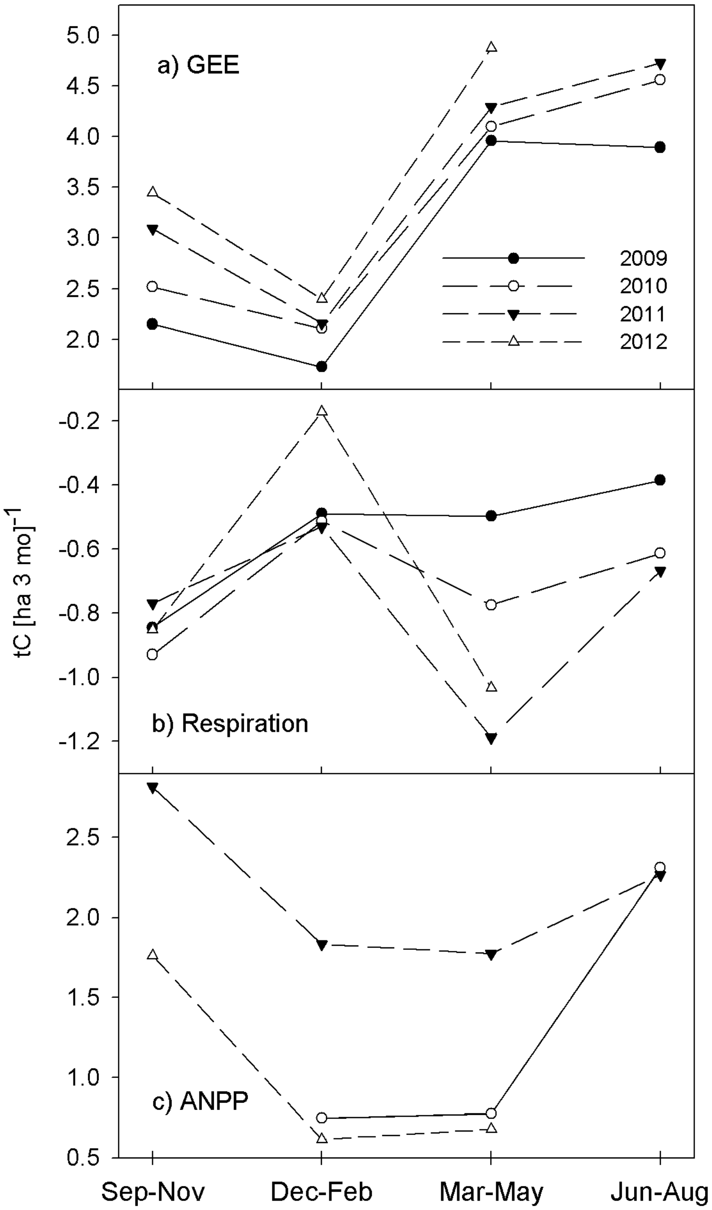

Figure 3.5. Seasonal carbon exchange from 2009 – 2012 in tC [3 mo]$^{-1}$. a) Gross ecosystem exchange, b) respiration, and c) aboveground net primary production.

3.3.3. Seasonality of CO_2 and H_2O exchange

Gross ecosystem exchange (uptake is positive), a measure of whole-forest photosynthesis, continued year round [Figure 3.5a, Figure 3.6a]. Gross ecosystem exchange was highest in spring and summer, averaging from 4.3-4.4 tC ha^{-1} [3 mo]$^{-1}$ for both seasons. Winter GEE was nearly half summer GEE, averaging 2.1 tC ha^{-1} [3 mo]$^{-1}$ for the season. Despite a persistent and deep snowpack, the forest showed photosynthetic activity and growth year round; winter accounted for 15% of annual total GEE, and winter GEE rates were similar to summer GEE rates at comparable temperatures [Figure 3.7]. Autumn months also showed high photosynthetic activity, despite a lack of substantial precipitation in the previous five to six months.

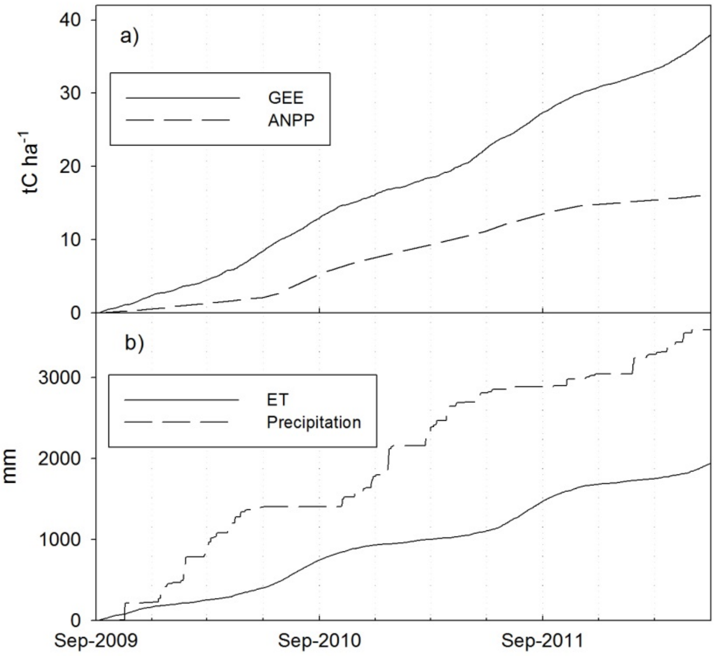

Figure 3.6. Cumulative carbon and water exchange from September 2009 to September 2012. a) GEE (solid line) and ANPP (dashed line), b) ET (solid line) and precipitation (dashed line).

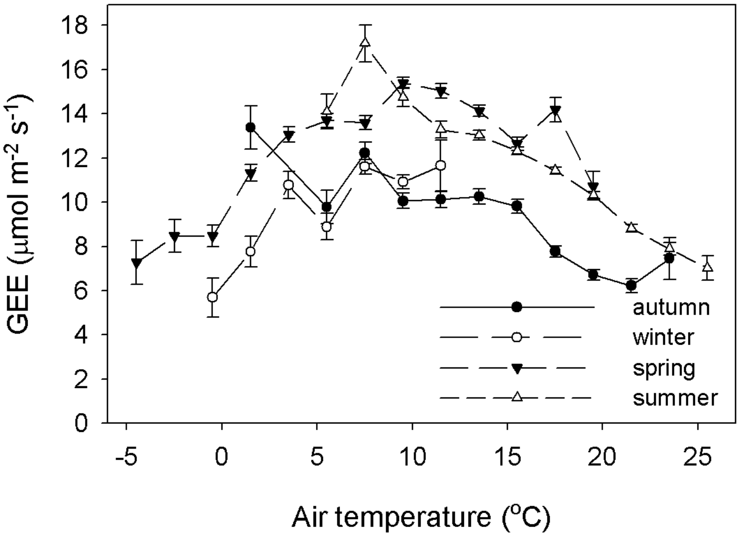

Figure 3.7. GEE response to temperature by season. Temperature is binned in 2°C increments, minimum 20 points per bin.

Evapotranspiration averaged 765 mm yr^{-1} (see also Goulden et al., 2012). Evapotranspiration was highest in summer, and summer ET accounted for 45% of the annual total [Figure 3.8a]. Spring ET accounted for 21% of the annual total, autumn accounted for 24% and winter accounted for 10%. The seasonal pattern of water use efficiency (WUE) was consistent from year to year [Figure 3.8b]. Water use efficiency (WUE) was defined as seasonally averaged half-hourly mean GEE (µmol CO_2) divided by mean ET (mmol H_2O^{-1}) during sunny periods (K > 600 W m^{-2}). Water use efficiency was highest in winter and spring, at about 3.9 mmol CO_2 mol H_2O^{-1}. Summer and autumn consistently showed low water use efficiency, from 2.0 – 2.5 mmol CO_2 mol H_2O^{-1} [Figure 3.8b].

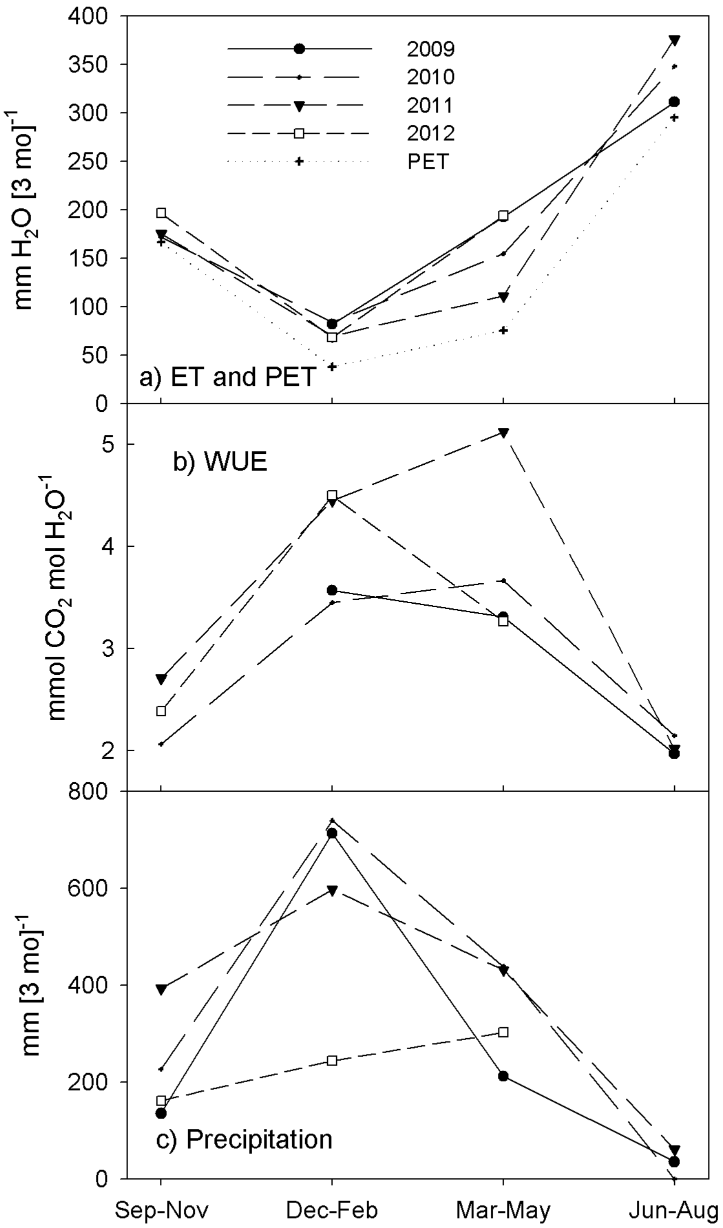

Figure 3.8. Seasonal water exchange. a) Total seasonal evapotranspiration (mm H_2O), dotted line is mean seasonal PET, b) mean seasonal water use efficiency during sunny periods (K > 600 W m^{-2}), c) total seasonal precipitation (mm H_2O).

Ecosystem light use efficiency (LUE) is a measure of photosynthetic carbon uptake per watt of absorbed incoming radiation. We calculated seasonal light use efficiency by summing seasonal gross ecosystem exchange and divided by seasonal total incoming solar radiation to understand how GEE was influenced by seasonal radiation [Figure 3.9]. Light use efficiency was highest in winter, slightly lower in spring, and lowest in summer. Autumn LUE was variable.

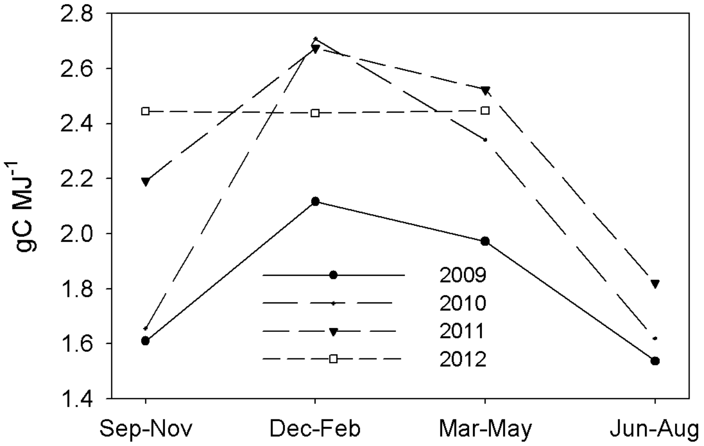

Figure 3.9. Mean seasonal grams of gross carbon uptake per incoming megajoule of solar radiation.

3.3.4. Canopy gas exchange responses to meteorological conditions

We compared the GEE rates during sunny periods (K > 600 W m^{-2}) with canopy air temperatures measured at the tower top to understand how winter cold and summer drought affect photosynthetic rates. Despite a small 2.0^{0}C difference in air temperature between summer and autumn sunny periods, we found that autumn GEE rates dropped by 25% compared to summer [Figure 3.5].

Mean GEE rates never dropped below 5.7 µmol CO_2 m^{-2} s^{-1} during sunny periods. Photosynthesis continued below air temperatures of 0^{0}C [Figure 3.7]. Spring GEE peaked around 10^{0}C at 15.4 µmol CO_2 m^{-2} s^{-1}, while GEE peaked around 8^{0}C during the rest of the year. Spring and summer showed almost identical temperature responses of GEE, except that summer

GEE was much higher in the 7-10^{0}C range than spring. Winter responses of GEE were depressed at a level similar to autumn. Winter cold acclimation would be evident as a less sensitive temperature response curve of GEE in winter compared to other seasons. Below 10 °C, we did not see a difference in response of GEE to cold temperatures [Figure 3.7]. ANCOVA analysis showed the slope of GEE response to cold temperature is identical between seasons ($p < 0.05$).

Gross ecosystem exchange declined with increasing canopy air temperatures above 12^{0}C in spring and summer. Autumn GEE declined with increasing canopy air temperatures above 15^{0}C. ANCOVA analysis showed the slope of GEE response to increasing temperatures above these thresholds is identical between spring, summer, and autumn ($p < 0.05$). Winter canopy air temperatures never rose above 12^{0}C, and at these temperatures no decline in GEE with warm temperature was observed.

We used surface soil data as a proxy for water content throughout the column and as a measure of the timing of the wet and dry seasons, but note that trees access soil water far below this depth [*Bales et al.*, 2011b; *Fellows and Goulden*, 2014]. Gross ecosystem exchange during sunny periods was well correlated with soil volumetric water content (VWC) in the upper 30 cm, especially below about 0.09 $cm^3\ cm^{-3}$. Gross ecosystem exchange was lowest in summer, when soil VWC dropped below 0.05 $cm^3\ cm^{-3}$, and highest in winter, when soil water climbed above 0.12 $cm^3\ cm^{-3}$. Autumn had the narrowest intraseasonal range and lowest values of soil VWC (~0.05 – 0.08 $cm^3\ cm^{-3}$), but showed moderate rates of GEE, around 11 $\mu mol\ CO_2\ m^{-2}\ s^{-1}$.

We tested the hypothesis that warm temperatures and dry soils during summer and autumn interact to depress GEE. Periods during the summer and autumn months above 12^{0}C were considered [Figure 3.7]. The influence on GEE of temperature, soil volumetric water content, and their interaction was evaluated using a multivariate linear model. Warming temperatures, drying soil moisture, and the interaction each significantly depress GEE during sunny periods ($p < 0.05$).

Mean annual ET was 765 mm yr^{-1}, while annual precipitation was 1102 mm yr^{-1} during the study period. The pattern of seasonal ET was out of phase with the pattern of precipitation: winter accounted for 10% of annual ET and 50% of annual precipitation, and summer accounted for 45% of annual ET and just 3% of annual precipitation [Figure 3.8].

3.4. Discussion

3.4.1. How does summer heat and drought limit forest canopy gas exchange?

Previous work has suggested the Sierran mixed conifer forest is limited by stress with both winter cold and summer drought [*Stephenson*, 1998; *Urban et al.*, 2000; *Royce and Barbour*, 2001b], yet our canopy CO_2 and H_2O flux measurements show high rates of canopy gas exchange continuously year-round, including periods with cold temperatures and summer drought. About 60% of annual GEE occurred during months when the ground was usually snow-covered and temperatures were close to freezing. The remaining 40% of annual GEE occurred during the dry season, when only 10% of annual precipitation fell. There was net carbon accumulation during all months of the year.

Photosynthesis rates remained high throughout the winter. During sunny periods, GEE rates in winter were 90% of summer rates, despite a mean air temperature of 6.7^{0}C. Below 12^{0}C, GEE declined with decreasing temperature at the same rate between summer and winter ($p < 0.05$), indicating no winter dormancy. Photosynthesis rates remained high through the late summer drought. Above 12^{0}C, photosynthesis decreased with increasing temperature at similar rates during summer and spring [Figure 3.7]. This indicates the sensitivity of leaf gas exchange to temperature, associated with either stomatal closure or reduced net CO_2 uptake, did not increase with summer drought. Late summer drought stress would be evident in diminishing evapotranspiration compared to potential evapotranspiration as the summer progresses. In the Sierra mixed conifer forest, evapotranspiration was nearly equal to potential evapotranspiration year round [Figure 3.8a]. This implies that drought stress did not induce dormancy in late summer and roots accessed moisture in the deeper soil and regolith.

3.4.2. Plant adaptation to avoid drought and cold stress

Four phenomena helped the vegetation avoid cold and drought limitation: 1) trees were adapted to photosynthesize at low temperatures, 2) air temperatures in the canopy were warmer in winter and cooler in summer compared to 2 m heights, 3) trees were able to access water during the winter freezing period, and 4) trees were able to access soil water through the summer drought period.

Cold temperatures during sunny periods did not strongly constrain annual net production, and this forest had a low optimal temperature for GEE [Figure 3.7]. Maximum GEE uptake occurred at an air temperature of about 8^0C and remained at 50% of maximum rates near 0^0C during all seasons. GEE was reduced by 50% or more due to cold during only 2% of sunny periods. At about 3^0C, NEE rates were more than 75% of peak rates in both spring and autumn.

The optimal temperature range for GEE in this forest was between about 5 and 13^0C, which is lower than almost all observed forest types reported by Yuan et al. (2011). The temperature below which NEE becomes a loss, T_b, was -6^0C in the Sierra mixed conifer forest. This is 5^0C lower than T_b at a mixed conifer site in Southern California, reported by Fellows and Goulden [2013]. The Sierra mixed conifer forest T_b was 13^0C below the value of $+8.2^0$C predicted by Yuan et al. [2011] for a forest with the same mean annual temperature.

We suspect there are four reasons for this apparent cold adaptation. The first is that leaf physiology was adapted to take advantage of winter precipitation and intermittent warm, sunny conditions during winter months: only 3% of sunny periods were below 0^{0}C. Second, the ecosystem rarely experienced temperatures below -5^{0}C (2.5% of the year) and thus leaves did not need protection against freezing or cold desiccation [*Parker*, 1963]. Third, the soils did not freeze and snow melted from below, which provided accessible soil water throughout the winter [*Bales et al.*, 2011b]. Finally, this forest was at 37^{0}N latitude. Midwinter days received enough radiation for net photosynthetic carbon uptake. Dark-colored leaves were likely several degrees warmer than air temperature. These factors together negated any advantage of winter dormancy, and there was no evidence of winter dormancy in any of the conifer species found at this site.

Canopy air temperatures were moderate compared to surface (2 m) air temperatures [Figure 3.4]. Summer daytime canopy VSD was less than surface VSD, and winter daytime canopy air temperatures were warmer than surface air temperatures. Rambo and North [2009] also found in nearby stands of mixed-conifer forest that winter temperatures were warmer in the canopy than at the surface, and summer mean daytime air temperatures were cooler in the canopy than at the surface. Moderate canopy temperatures were advantageous for tall trees compared to shorter vegetation: evaporative demand was diminished in summer and higher photosynthetic rates were possible in winter.

Mean seasonal GEE showed a limited response to soil moisture. Summer and autumn were consistently dry, but autumn GEE was diminished by only about 20% compared to spring. This forest experienced a slowdown in photosynthesis when surface soil VWC dropped below about 0.07, suggesting a threshold for a limited physiological response to drought stress caused by low soil surface VWC, and exacerbated by increasing temperature. This response was only substantial during the dry season, several months after snow has melted and before winter rains arrived.

3.4.3. Why has the effect of drought and cold been overestimated?

Physiology and production in this forest were neither greatly cold-limited in winter nor drought-limited in summer. Discussions of natural history [*Waring and Franklin*, 1979; *Stephenson*, 1988; *Schoenherr*, 1992; *Urban et al.*, 2000; *Walter and Breckle*, 2002] suggest that Sierra montane forest experiences a substantial water deficit in late summer and an energy deficit in mid-winter. These limitations would cause summer drought stress and winter dormancy in this forest, constraining growth to narrow seasonal windows, and potentially resulting in low annual production and biomass. However, standing biomass in this forest was large, comparable to tropical rainforests [*Houghton*, 2005]. Net primary production was also comparable to tropical forests [*Clark et al.*, 2001], and stem growth occurred year round. We identified two environmental factors moderate the effects of cold winters and dry summers: 1) moderate canopy air temperatures, and 2) accessibility of deep soil water.

Canopy air temperatures above about 10 m were moderate compared to temperatures near the surface [Figure 3.4]. Winter temperatures above 10 m were 1.9^{0}C warmer at night compared to 2 m temperatures. Summer daytime temperatures were 2.6^{0}C cooler above 10 m compared to 2 m temperatures, and summer night-time temperatures were 2.1^{0}C warmer above 10 m. Many models of photosynthesis and evapotranspiration rely on measured or estimated air temperatures at 2 m height. Air temperatures at 2 m height were warmer in summer and colder in winter than canopy air temperatures. This incorrect estimation of canopy meteorology could cause models to overestimate summer evapotranspiration and drought stress as well as winter cold limitation on photosynthesis.

The Mediterranean mixed conifer forest supports high standing biomass, and is thus expected to exhibit drought stress and drought avoidance strategies to avoid embolism and carbon starvation during the long summer dry period [*Panek and Goldstein*, 2001]. Spring and autumn temperatures were nearly identical, but soils were mostly saturated in spring whereas the upper 1-2 m was completely dry in autumn. Our data show a modest 11% reduction in GEE rates in autumn compared to summer despite a lack of substantial precipitation for the prior several months. The slight reduction in GEE and similar WUE between summer and autumn indicate the forest is accessing deep soil water throughout the dry season.

3.4.4. Implications for impacts of climate change

Models of the impact of a changing climate on the Sierra Nevada that rely on the assumption that productivity in the mid-montane forest is limited by winter cold and summer drought may be predict inaccurate responses. The Sierra mixed conifer forest is well-adapted to its present environmental conditions. Trees growing at the site accessed deep soil water during summer and autumn, mitigating potential drought stress [*Bales et al.*, 2011b]. The mixed conifer forest avoided winter dormancy and took advantage of the ample soil water and slightly-above-freezing temperatures of winter.

The high year round rates of GEE, a stable year round WUE, seasonal ET equal to PET, and a high ET:P ratio lead us to conclude that annual ET is co-limited by precipitation and potential evapotranspiration. While this forest was suited to current meteorological norms, this analysis also suggests vulnerabilities to future drought and warming. This forest lost the majority of its annual precipitation through evapotranspiration [Figure 3.6b]. If droughts intensify in the region as predicted [*Cayan et al.*, 2008; *Diffenbaugh et al.*, 2008], this forest would draw down deep soil water earlier in the summer and experience longer and more intense drought stress during summer and autumn. Decreased available water would support less vegetation, cause forest mortality, and decrease standing biomass and annual production episodically during drought years.

Predicted warming with no change in precipitation would also intensify drought stress in two major ways. Higher temperatures will increase PET and evapotranspiration rates, drawing down deep soil water earlier in the season and exacerbating late summer drought stress. Additionally, the winter snowpack allows deep percolation of water into soil weeks after the last precipitation, reducing the length of the dry season in the soil [*Winograd et al.*, 1998]. Snow at the site often fell at temperatures very close to freezing; with slight warming, winter precipitation will arrive as rain. This will reduce water stored in soils and lengthen the period between soil water input in spring and fall. The combination of increased ET and decreased soil water would force the forest to reduce its vegetation density, thereby reducing biomass and annual production.

Chapter 4. Water use efficiency variability and controls across ten California ecosystems

4.1. Introduction

Ecosystem carbon and water cycling are connected by water use efficiency (WUE). Photosynthetic uptake of carbon requires opening stomata that allows water loss via evapotranspiration (ET). Plants employ a wide variety of adaptive mechanisms to minimize the tradeoff between carbon gain and water loss given environmental conditions [*Osmond et al.*, 1987], including stomatal control [*Cowan and Farquhar*, 1977], photosynthetic pathways [*Nobel and Jordan*, 1983], and overall photosynthetic capacity [*Sharkey*, 1984].

California's Mediterranean climates span a broad temperature range, from the Colorado Desert to the alpine peaks of Sierra Nevada Mountains. Timing of precipitation compared to favorable growing temperature varies dramatically within this range, and is a factor in creating the wide diversity of ecosystem types found there [*Barbour et al.*, 2007]. Precipitation regimes across California are predicted to change in the future toward increased drought intensity and warming [*Cayan et al.*, 2010]. Understanding the meteorological controls and physiological limits on water use efficiency can indicate the adaptability of these ecosystems to environmental change.

Ecosystem water use efficiency (WUE) can be calculated as the ratio of gross primary production to evapotranspiration. Evapotranspiration at the ecosystem level is the product of a number of interrelated factors, including water lost to surface evaporation [*Grelle et al.*, 1997; *Wilson et al.*, 2001], vapor pressure deficit [*Monteith*, 1965], and canopy conductance [*Kelliher et al.*, 1993]. In this study, we examine the contribution of each of these factors to evapotranspiration at ten sites across a precipitation gradient in California.

4.2. Methods

We evaluated the relationships between WUE, meteorology, and ecosystem physiology across a diverse set of ecosystems and climates to understand the controls on ecosystem water use efficiency. We focused on ten California ecosystems across a 1200 mm yr^{-1} precipitation gradient [Table 4.1]. Six sites span a 100 km east-west, coast-to-desert transect in Southern California. Four sites span a 70 km east-west, 2300 m elevation transect in the central Sierra Nevada Mountains of California [*Kelly and Goulden*, 2014]. An eddy covariance tower at each site measured carbon flux, water vapor flux, sensible heat flux, and meteorology [*Goulden et al.*, 1996]. Aboveground biomass and net primary productivity were measured at nine of the ten sites.

Table 4.1. Site ecosystem types, locations, mean annual temperature (MAT) and mean annual precipitation (MAP).

	Elevation (m)	Latitude (^{0}N)	Longitude (^{0}W)	MAT (^{0}C)	MAP (mm)
Desert scrub	275	33.652	-116.372	23.2	114
Desert chaparral	1300	33.610	-116.450	16.4	287
Pinyon-juniper woodland	1280	33.605	-116.455	16.5	287
Coastal grassland	470	33.737	-117.695	16.5	288
Coastal sage scrub	475	33.734	-117.696	16.4	288
Oak-mixed conifer forest	1710	33.808	-116.772	13.2	429
Oak savannah	405	37.109	-119.731	17.6	536
Ponderosa forest	1160	37.031	-119.256	14.0	808
Sierra mixed conifer forest	2015	37.067	-119.195	9.0	943
Lodgepole forest	2700	37.067	-118.987	4.9	1368

Gross primary production (GPP) was computed by summing the half-hourly CO_2 fluxes calculated from the eddy covariance tower measurement. Annual ET was calculated by filling and summing half-hourly water vapor fluxes. Net radiation was fit to the sum of latent heat, sensible heat, and soil heat fluxes to calculate energy budget closure. Water and CO_2 fluxes were corrected by this energy budget closure term.

Water use efficiency (WUE) was calculated as annual gross primary production (GPP) divided by annual evapotranspiration (ET;

Equation 4.1).

Equation 4.1. Ecosystem WUE.

$$WUE = \frac{GPP}{ET}$$

Vapor pressure deficit (VPD) and canopy conductance (G_s) were calculated using an inverted Penman-Monteith method [*Stewart*, 1988]. The ratio of internal leaf to external CO_2 partial pressures was calculated with

Equation 4.2.

Equation 4.2. Canopy c_i/c_a.

$$\frac{c_i}{c_a} = 1 - \frac{GEE \cdot p_a}{G_s \cdot c_a}$$

Surface evaporation is a component of evapotranspiration that never enters the ecosystem. Greater surface evaporation relative to transpiration would reduce ecosystem WUE, despite the ecosystem never accessing to this water. We quantified the magnitude of surface evaporation by calculating ET while snow was on the ground or within 72 hours following rain (ET_{wet}) with ET calculated during all other periods (ET_{dry}). We fit ET_{dry} to incoming solar radiation and used this fit to estimate ET_{dry} during wet periods. Estimations of ET_{dry} were subtracted from ET_{wet} during wet periods to obtain the difference in ET between wet and dry periods. We attribute the difference between ET_{wet} and ET_{dry} to surface evaporation. The sum of the excess ET during wet periods was divided by total annual ET to estimate the fraction of total annual ET lost to surface evaporation [Figure 4.2a].

4.3. Results and Discussion

Water use efficiency increased with increasing annual precipitation up to about 600 mm yr^{-1} [Figure 4.1a]. Water use efficiency plateaued above 600 mm yr^{-1}, at around 2.5 mol H_2O [mmol CO_2]$^{-1}$. Interannual variability in WUE at nine of the ten sites was less than the variability in WUE between sites. Grasslands, shrublands, and savannah (including the pinyon-juniper site) showed increased WUE with increased precipitation. Montane conifer forests, where average annual precipitation was above 600 mm yr^{-1}, experienced slight or no increase in WUE during drier years.

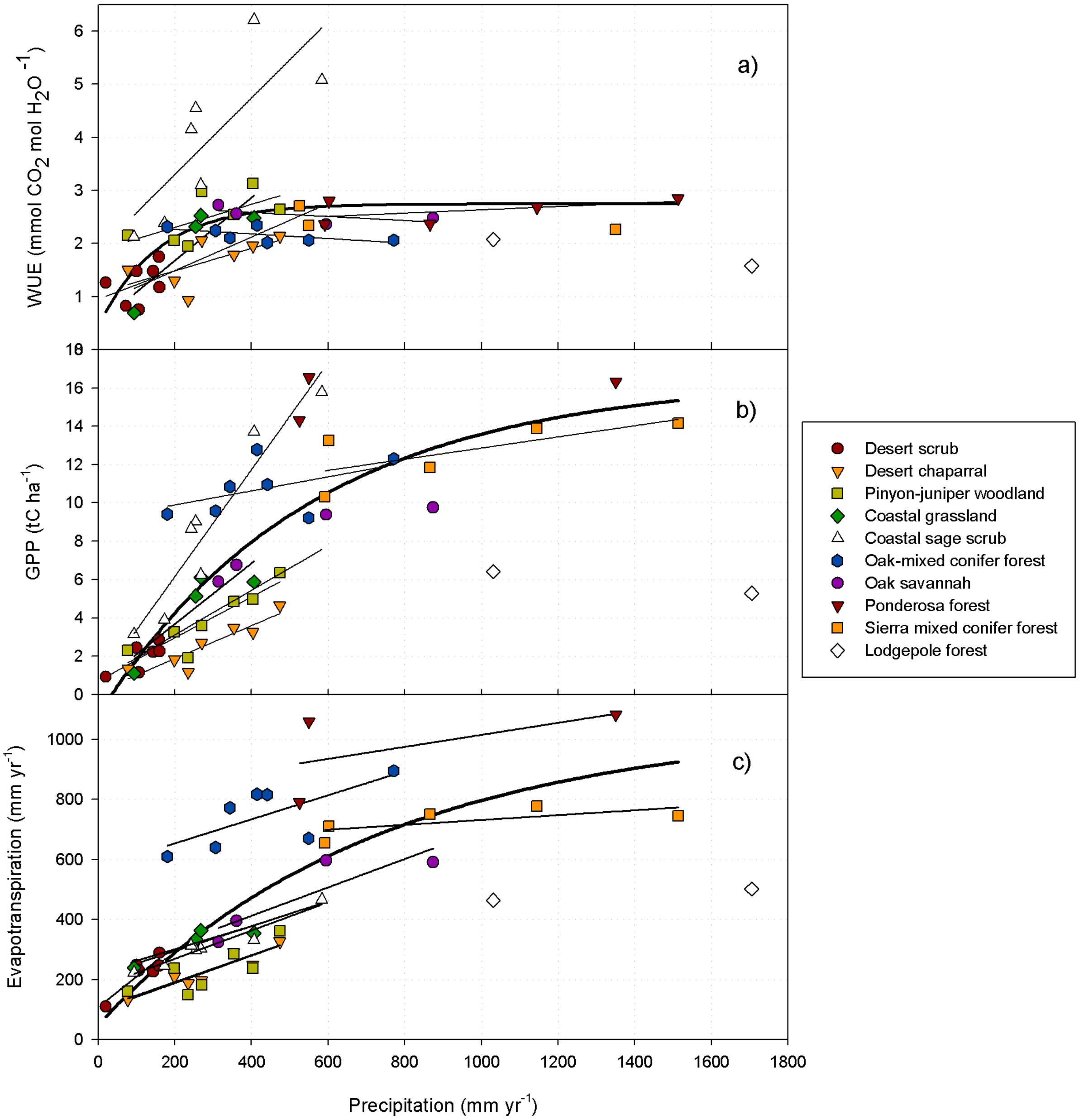

Figure 4.1. Ecosystem water use efficiency, gross primary production, and evapotranspiration with respect to annual precipitation. Thin lines are linear fits of variables vs. annual precipitation at each site. Bold lines are inverse exponential fits to all sites excluding lodgepole forest. a) Annual water use efficiency (WUE; mmol CO_2 [mol H_2O]$^{-1}$). b) Gross primary production in tC ha^{-1}. c) Evapotranspiration in mm yr^{-1}.

Gross primary production increased more rapidly than ET with increased precipitation [Figure 4.1a,b], causing the steep curve in WUE below 400 mm yr^{-1}. Above about 600 mm yr^{-1}, both GPP and ET increased at similar rates with precipitation, which caused a plateau in WUE.

The distribution of annual WUE with precipitation raises four questions: 1) what determines the steep slope of WUE below 600 mm yr^{-1} and the plateau of WUE above 600 mm yr^{-1}, 2) what determines interannual variability in WUE within sites, 3) why is WUE at the coastal sage scrub site much higher than the overall trend, and 4) why is the WUE at the lodgepole site below the overall trend? We examine three major components of WUE to answer these questions: 1) the surface evaporation fraction of evapotranspiration, 2) meteorological drivers of evapotranspiration, and 3) plant physiological control of evapotranspiration.

4.3.1. Surface evaporation control on ecosystem water use efficiency

Ecosystem water use efficiency across all sites and all years generally declined with increasing fraction of ET lost to surface evaporation [Figure 4.2a]. Warmer and drier sites lost the highest fraction of ET to surface evaporation [Figure 4.2b]. We attribute greater surface evaporation at these sites to warmer temperatures following rain and less canopy closure at these sites [*Jin and Goulden*, 2013], which is associated with increased surface evaporation [*Black and Kelliher*, 1989].

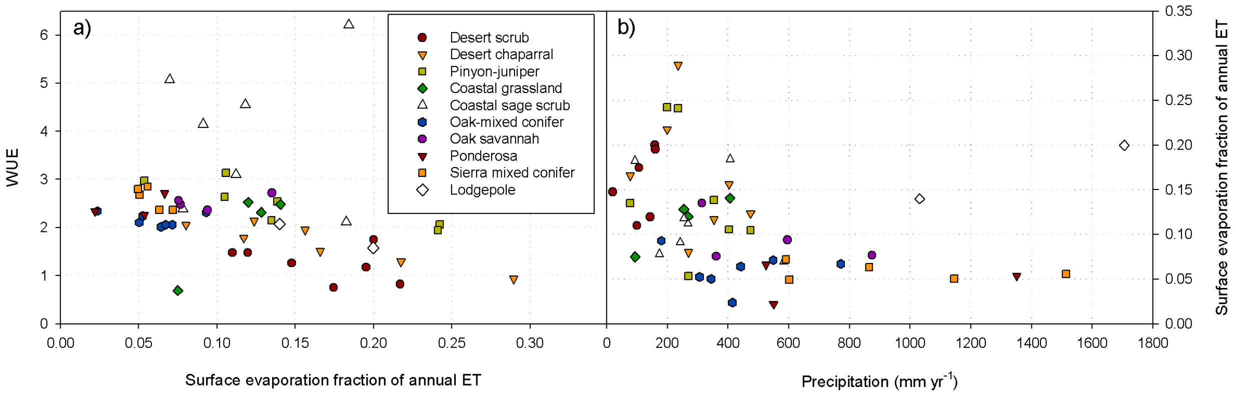

Figure 4.2. Surface evaporation. a) Annual WUE as a function of fraction of ET lost to surface evaporation. b) Surface evaporation fraction of ET as a function of annual precipitation.

4.3.2. Meteorological control of WUE

Vapor pressure deficit is an important driver of evapotranspiration. We calculated half-hourly VPD for sunny periods (K > 400 W m^{-2}) using tower meteorological data and leaf temperature inferred using an inverted Penman-Monteith equation. Half-hourly VPD was then weighted by half-hourly GEE to obtain a weighted VPD$_{GEE}$. Ecosystem WUE was compared to VPD$_{GEE}$ [Figure 4.3].

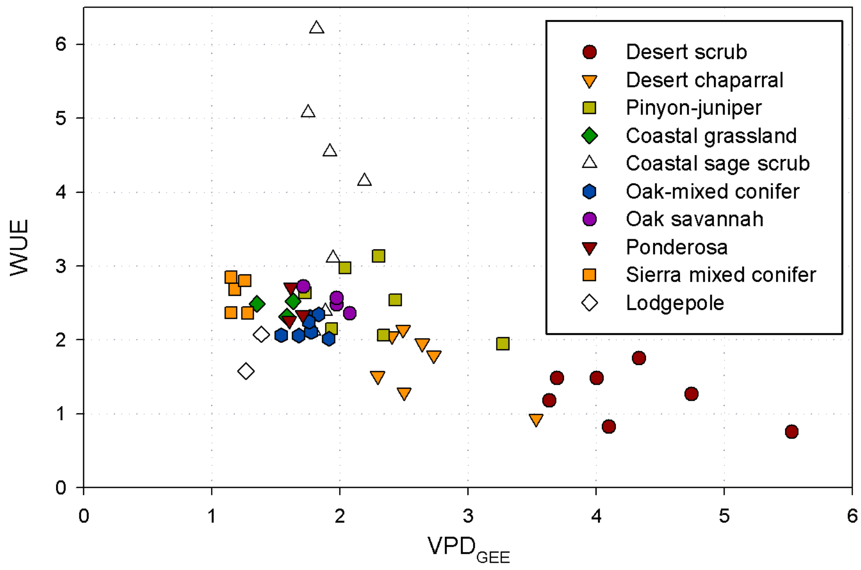

Figure 4.3. Annual WUE vs. VPD (kPa) weighted by half-hourly GEE during sunny periods (K > 400 m^{-2}).

The broad trend was a general decline of WUE with increasing VPD$_{GEE}$. Montane conifer ecosystems exhibited no response of WUE to VPD$_{GEE}$. Decreasing WUE with increasing Montane sites clustered within a narrow range of VPD$_{GEE}$ from 1.0 – 2.0 and WUE from 2.0 – 3.0, and none exhibited clear trends in WUE with VPD$_{GEE,}$ suggesting that VPD is not an important control on WUE at these sites. The coastal sites did not exhibit a large interannual variability in VPD$_{GEE}$ and could not explain the high WUE at the sage site. VPD$_{GEE}$ at the three desert sites matches the prediction of decreasing ecosystem WUE with increasing VPD [*Jarvis and McNaughton*, 1986]. Vapor pressure deficit, when weighted by half-hourly GEE, is an important control on WUE in only the desert systems.

4.3.3. Physiological control on ecosystem water use efficiency

Mean annual canopy internal CO_2 concentrations exhibit strong interannual variability at the desert, scrubland, and savannah sites, but no significant variability at the montane sites [Figure 4.4]. The desert, coastal, and savannah sites are composed of mixes of annuals, perennials, forbs, grasses, shrubs, and small trees. The flexible physiology of desert and Mediterranean shrubs can lead to high interannual variability of ecosystem-level c_i/c_a [*Ehleringer et al.*, 1991, 1992]. The montane sites are composed largely of evergreen trees with few C_4 and annual plants. The montane sites were buffered from drought stress, likely due to deep rooting, which minimized the effects of low rain years on c_i/c_a [*Fellows and Goulden*, 2013, 2014; *Kelly and Goulden*, 2014; *Kelly et al.*, 2014].

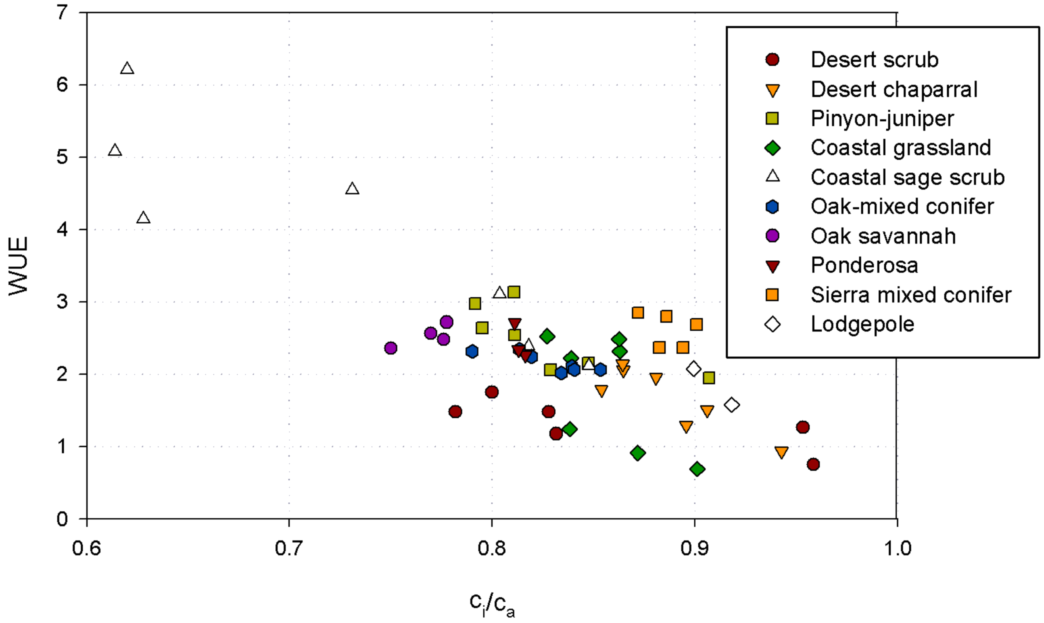

Figure 4.4. WUE vs c_i/c_a during sunny periods ($K > 400$ W m^{-2}) with moderate VPD (0.5 - 3.0 kPa).

Increasing c_i/c_a is associated with decreasing WUE at eight of the ten sites, consistent with theory relating WUE to c_i/c_a [*Field et al.*, 1983]. The oak woodland exhibited an opposite trend, with low interannual variability in c_i/c_a. Coastal sage scrub annual mean c_i/c_a varied 50%, the widest range of c_i/c_a of the ten sites. Interannual variability in c_i/c_a in the montane conifer sites was lower than the desert and coastal sites, likely reflecting the greater water availability at the conifer sites.

4.3.4. Synthesis

The steep slope of WUE below 600 mm yr^{-1} precipitation is due to several complementary factors: high surface evaporation, high VPD_{GEE}, and responsive c_i/c_a. The driest sites show a significant decrease in WUE due to losses of precipitation to surface evaporation. Vapor pressure deficit is also an important limiting factor on WUE in dry ecosystems: above VPD_{GEE} of 2.0 kPa, all ecosystems showed a decline in WUE with increasing VPD_{GEE}. Increasing c_i/c_a was associated with a decline in water use efficiency at nine of the ten sites.

Interannual variability in WUE between sites was only observed at the driest sites, below annual precipitation of 600 mm yr^{-1}. These sites all exhibited the greatest interannual variability in surface evaporation, VPD_{GEE}, and c_i/c_a, leading to more variability in annual WUE. Interannual variability in WUE at the montane conifer sites was insignificant; these sites showed little variability in surface evaporation, VPD_{GEE}, and c_i/c_a.

The coastal sage scrub site stands apart from the other sites with four years of WUE more than double the mean WUE of other sites. The effect of VPD_{GEE} had little effect on WUE. Years with lower surface evaporation had higher WUE, but the most important factor was c_i/c_a. During the four years with very high WUE, c_i/c_a was lower than any other site. This site was recovering from a fire immediately preceding the study period, and coincident above-average rainfall. The site biomass and production was dominated by *Acmispon glaber* ((VOGEL) BROUILLET), a nitrogen fixer. *A. glaber* maintains low c_i/c_a [*Comstock and Ehleringer*, 1986] and N-fixers exhibit higher WUE compared to non-N-fixing C3 plants [*Sage and Pearcy*, 1987]. We conclude the high WUE at the coastal sage site was due to post-fire recovery dominated by a nitrogen fixer during a period of high rainfall.

The lodgepole site shows WUE below the mean WUE for other montane conifer sites. This site's surface evaporation rate, VPD_{GEE}, and c_i/c_a were within the ranges of the other conifer sites, suggesting a fourth control on its low WUE. Annual GPP was about half of GPP at other conifer sites with similar precipitation, and this was the only site that experienced prolonged winter dormancy [*Kelly and Goulden*, 2014]. We conclude that the low annual GPP due to winter dormancy is the cause of low annual WUE at this site.

4.4. Conclusions

This study highlights the variability of sensitivities to important controls on water use efficiency. Dry ecosystems ($P < 600$ mm yr^{-1}), composed of a mix of annual grasses, forbs, and drought-adapted shrubs, can respond more flexibly to interannual variability in precipitation. Variability in annual precipitation can cause significant changes in leaf area and species composition, and a concomitant change in WUE. In contrast, wetter ecosystems ($P > 600$ mm yr^{-1}) are composed of long-lived, high biomass trees. These forests contain biological inertia: they are unable to alter leaf area or species composition in response to a single drought year, and thus WUE is insensitive to interannual variability in precipitation.

Chapter 5. Conclusions

This dissertation attempted to better understand how climate affects carbon balance, water cycling, and ultimately ecosystem function. Chapter two examines a climate gradient across the Sierra Nevada to quantify the climate limitations on growth and the controls on biomass. Chapter three focuses on the ecophysiology of the mixed conifer forest of the Sierra Nevada to understand ecosystem vulnerabilities and resilience to winter cold and summer drought. Chapter four is an analysis of ten diverse ecosystems to understand how climate controls the interactions between gross primary production and water use, and to parse the components of evapotranspiration.

5.1. Chapter synopses

Chapter two builds an understanding of how climate limits growing season, photosynthesis rates, and ultimately governs ecosystem carbon storage. The western slope of the Sierra Nevada was the study system: four eddy covariance towers measured meteorology, gas fluxes, and energy balance over a 2300 m elevation range. Ecosystem production was also observed via ground-based measurements. The length of the growing season, mortality rates, and timing of favorable temperatures with respect to available soil water were the primary drivers of ecosystem type and standing biomass. The subalpine site could become more productive with warming or drought due to a longer growing seasons. The other sites would likely lose biomass with increased mortality, and the ponderosa forest may be the most vulnerable to type conversion with warming or drought, to lower-biomass, drought tolerant chaparral.

Chapter three is an analysis of seasonal cold- and drought-induced limitations on productivity in the Sierra mixed conifer forest. This region has an anomalously high biomass and production for a montane Mediterranean climate, based on bioclimatic conceptual models. The observations presented show that the snowy winters did not induce winter dormancy, nor did summer drought strongly curtail late summer photosynthesis. The growing season at this site was nearly year-round, and was limited primarily by available solar radiation during short winter days and cloudy winter storms. Low-temperature photosynthesis and access to deep soil water appear to be the main mechanisms that allow this forest to persist.

Chapter four compares the relationship of ecosystem water use efficiency to climate across ten major ecosystem types in California. Water use efficiency was positively correlated with precipitation below 600 mm yr^{-1} and plateaus above this threshold. High vapor pressure deficit, high surface evaporation, and high internal CO_2 concentrations at the desert and coastal sites both contributed lower WUE, but did not affect the montane forest sites. Lower annual precipitation was associated with higher variability in ecophysiology, while montane conifer sites with high precipitation (above 600 mm yr^{-1}) exhibited inflexible ecophysiological response to interannual variability in precipitation.

5.2 Implications and future directions

These results highlight the need for an understanding of climatic thresholds of ecophysiological response across individual ecosystem functional types. These analyses show that nearby ecosystem types can exhibit vastly different adaptations and responses of growth, water use, and dormancy to changes in temperature and precipitation. Recognizing ecosystems close to their physiological limits of survival is key to identifying the ecosystems most vulnerable to climate change.

These observations show that it is likely that low-elevation forests, which are already limited by summer drought and heat, would be the most vulnerable to a few degrees of warming or increased drought frequency. Ecosystems that are particularly well drought-adapted, such as coastal grassland, deserts, and oak savannah, would likely remain within their physiological limits with predicted warming and drought. California mid-montane forests could experience decreased biomass, perhaps similar to the recent forest mortality in the Rocky Mountains. Subalpine forests limited by cold temperatures and a persistent snowpack could increase their productivity and biomass with warming or drought.

This research could be improved with direct physiological measurements across the gradient, particularly leaf gas exchange and sap flux. Targeted measurements of individual trees of major species at a more refined elevational scale, at 100 to 200 m elevation increments, would illuminate stressors on species caused by climate. This study aggregated tree response at the plot level, but did not address species-level differences in physiology. These results show that physiological differences at the plot level are important, but identification of major species' contributions to carbon and water cycling would be critical to understand future consequences for ecosystem composition and species conservation.

California has undergone decades of severe drought and warmer temperatures in the Holocene, yet has remained the sole refuge of many species since the Pleistocene [*Raven and Axelrod*, 1995]. Vegetation mortality and range contraction are not the only possible outcome of future change. Understanding the vulnerability and resilience of California's unique communities is critical to predict the effect of future climate changes within the region, and will also provide a more nuanced understanding of ecophysiology that could aid predictions of terrestrial feedbacks to climate change globally.

Bibliography

Abatzoglou, J. T., K. T. Redmond, and L. M. Edwards (2009), Classification of regional climate variability in the state of California, *J. Appl. Meterology Climatol.*, *48*, 1527–1541.

Allen, C. D. et al. (2010), A global overview of drought and heat-induced tree mortality reveals emerging climate change risks for forests, *For. Ecol. Manage.*, *259*(4), 660–684, doi:10.1016/j.foreco.2009.09.001.

Araujo, M. B., and A. T. Petersen (2012), Uses and misuses of bioclimatic envelope modeling, *Ecology*, *93*(7), 1527–1539.

Bales, R. C., J. J. Battles, Y. Chen, M. H. Conklin, E. Holst, K. L. O'Hara, P. Saksa, and W. Stewart (2011a), *Forests and Water in the Sierra Nevada: Sierra Nevada Watershed Ecosystem Enhancement Project*, Merced, CA.

Bales, R. C., J. W. Hopmans, A. T. O'Geen, M. Meadows, P. C. Hartsough, P. Kirchner, C. T. Hunsaker, and D. E. Beaudette (2011b), Soil Moisture Response to Snowmelt and Rainfall in a Sierra Nevada Mixed-Conifer Forest, *Vadose Zo. J.*, *10*(3), 786, doi:10.2136/vzj2011.0001.

Barbour, M. G., T. Keeler-Wolf, and A. A. Schoenherr (2007), *Terrestrial Vegetation of California*, 3rd ed., edited by M. G. Barbour, T. Keeler-Wolf, and A. A. Schoenherr, University of California Press.

Barnett, T. P., J. C. Adam, and D. P. Lettenmaier (2005), Potential impacts of a warming climate on water availability in snow-dominated regions., *Nature*, *438*(7066), 303–9, doi:10.1038/nature04141.

Bergengren, J. C., D. E. Waliser, and Y. L. Yung (2011), Ecological sensitivity: a biospheric view of climate change, *Clim. Change*, *107*(3-4), 433–457, doi:10.1007/s10584-011-0065-1.

Black, T. A., and F. M. Kelliher (1989), Processes controlling understorey evapotranspiration, *Philos. Trans. R. Soc. B Biol. Sci.*, *324*(1223), 207–231, doi:10.1098/rstb.1989.0045.

California Department of Water Resources (2005), Volume 1: Strategic Plan, in *California Water Plan, Update 2005*, Department of Water Resources, Sacramento.

Campbell, J. E., D. B. Lobell, and C. B. Field (2009), Greater transportation energy and GHG offsets from bioelectricity than ethanol, *Science (80-.).*, *324*(5930), 1055–7, doi:10.1126/science.1168885.

Cayan, D. R. (1996), Interannual climate variability and snowpack in the Western United States, *J. Clim.*, *9*, 928–948.

Cayan, D. R., E. P. Maurer, M. D. Dettinger, M. T. Tyree, and K. Hayhoe (2008), Climate change scenarios for the California region, *Clim. Change*, *87*(S1), 21–42, doi:10.1007/s10584-007-9377-6.

Cayan, D. R., T. Das, D. W. Pierce, T. P. Barnett, M. T. Tyree, and A. Gershunov (2010), Future dryness in the southwest US and the hydrology of the early 21st century drought, *Proc. Natl. Acad. Sci. U. S. A.*, *107*(50), 21271–6, doi:10.1073/pnas.0912391107.

Chapin III, F. S., M. S. Torn, and M. Tateno (1996), Principles of Ecosystem Sustainability, *Am. Nat.*, *148*(6), 1016–1037.

Clark, D. A., S. Brown, D. W. Kicklighter, J. Q. Chambers, J. R. Thomlinson, J. Ni, and E. A. Holland (2001), Net primary production in tropical forests: an evaluation and synthesis of existing field data, *Ecol. Appl.*, *11*(2), 371–384.

Comstock, J. P., and J. R. Ehleringer (1986), Photoperiod and photosynthetic capacity in Lotus scoparius, *Plant, Cell Environ.*, *9*, 609–612.

Cowan, I. R., and G. D. Farquhar (1977), Stomatal function in the regulation of gas exchange, in *Society for Experimental Biology Symposium*, edited by D. H. Jennings, pp. 471–505, Society for Experimental Biology, Cambridge.

Das, A. J., N. L. Stephenson, A. L. Flint, T. Das, and P. J. van Mantgem (2013), Climatic correlates of tree mortality in water- and energy-limited forests, edited by G. Bohrer, *PLoS One*, *8*(7), e69917, doi:10.1371/journal.pone.0069917.

Dettinger, M. D., D. R. Cayan, M. K. Meyer, and A. E. Jeton (2004), Simulated hydrologic responses to climate variations and change in the Merced, Carson, and American River basins, Sierra Nevada, California, 1900-2099, *Clim. Change*, *62*(1), 283–317.

Diffenbaugh, N. S., F. Giorgi, and J. S. Pal (2008), Climate change hotspots in the United States, *Geophys. Res. Lett.*, *35*(16), 1–5, doi:10.1029/2008GL035075.

Dixon, R. K., S. Brown, R. A. Houghton, A. M. Solomon, M. C. Trexler, and J. Wisniewski (1994), Carbon pools and flux of global forest ecosystems, *Science (80-.).*, *263*, 185–190.

Eagan, S. M., C. T. Hunsaker, C. R. Dolanc, M. E. Lynch, and C. R. Johnson (2007), Discharge and Sediment Loads at the Kings River Experimental Forest in the Southern Sierra Nevada of California, in *Advancing the Fundamental Sciences, Section 2. Experimental and Research Watersheds*, pp. 217–224, US Department of Agriculture, Forest Service.

Ehleringer, J. R., S. L. Phillips, W. S. F. Schuster, and D. R. Sandquist (1991), Differential utilization of summer rains by desert plants, *Oecologia*, *88*(3), 430–434, doi:10.1007/BF00317589.

Ehleringer, J. R., S. L. Phillips, and J. P. Comstock (1992), Seasonal variation in the carbon isotopic composition of desert plants, *Funct. Ecol.*, *6*(4), 396–404.

Fellows, A. W., and M. L. Goulden (2012), Rapid vegetation redistribution in Southern California during the early 2000s drought, *J. Geophys. Res.*, *117*(949), G03025, doi:10.1029/2012JG002044.

Fellows, A. W., and M. L. Goulden (2013), Controls on gross production by a semiarid forest growing near its warm and dry ecotonal limit, *Agric. For. Meteorol.*, *169*, 51–60, doi:10.1016/j.agrformet.2012.10.001.

Fellows, A. W., and M. L. Goulden (2014), The controls on regolith water use in montane California, *'In Prep.*

Field, C. B., J. Merino, and H. A. Mooney (1983), Compromises between water-use efficiency and nitrogen-use efficiency in five species of California evergreens, *Oecologia*, *60*(3), 384–389, doi:10.1007/BF00376856.

Field, C. B., J. T. Randerson, and C. M. Malmstrom (1995), Global Net Primary Production: Combining Ecology and Remote Sensing, *Remote Sens. Environ.*, *51*, 74–88.

Field, C. B., D. B. Lobell, H. A. Peters, and N. R. Chiariello (2007), Feedbacks of Terrestrial Ecosystems to Climate Change, *Annu. Rev. Environ. Resour.*, *32*(1), 1–29, doi:10.1146/annurev.energy.32.053006.141119.

Flint, L. E., and A. L. Flint (2012), Downscaling future climate scenarios to fine scales for hydrologic and ecological modeling and analysis, *Ecol. Process.*, *1*(1), 2, doi:10.1186/2192-1709-1-2.

Foken, T. (2008), The energy balance closure problem: An overview, *Ecol. Appl.*, *18*(6), 1351–1367.

George, M., J. W. Bartolome, N. McDougald, M. Connor, C. Vaughn, and G. Markegard (2001), *Annual Range Forage Production*, Davis, California.

Goulden, M. L., J. W. Munger, S.-M. Fan, B. C. Daube, and S. C. Wofsy (1996), Measurements of carbon sequestration by long-term eddy covariance: methods and a critical evaluation of accuracy, *Glob. Chang. Biol.*, *2*(3), 169–182, doi:10.1111/j.1365-2486.1996.tb00070.x.

Goulden, M. L., S. D. Miller, H. R. da Rocha, M. C. Menton, H. C. De Freitas, A. M. e Silva Figueira, and C. A. D. de Sousa (2004), Diel and seasonal patterns of tropical forest CO2 exchange, *Ecol. Appl.*, *14*(4), S42–S54, doi:10.1890/02-6008.

Goulden, M. L., R. G. Anderson, R. C. Bales, A. E. Kelly, M. Meadows, and G. C. Winston (2012), Evapotranspiration along an elevation gradient in California's Sierra Nevada, *J. Geophys. Res.*, *117*(G3), G03028, doi:10.1029/2012JG002027.

Grelle, A., A. Lundberg, A. Lindroth, A.-S. Morén, and E. Cienciala (1997), Evaporation components of a boreal forest: variations during the growing season, *J. Hydrol.*, *197*(1-4), 70–87, doi:10.1016/S0022-1694(96)03267-2.

Guisan, A., and W. Thuiller (2005), Predicting species distribution: offering more than simple habitat models, *Ecol. Lett.*, *8*(9), 993–1009, doi:10.1111/j.1461-0248.2005.00792.x.

Hall, R. C. (1944), A vernier tree-growth band, *J. For.*, 742–743.

Hinzman, L. D. et al. (2005), Evidence and Implications of Recent Climate Change in Northern Alaska and Other Arctic Regions, *Clim. Change*, *72*(3), 251–298, doi:10.1007/s10584-005-5352-2.

Holdridge, L. R. (1967), *Life zone ecology*, Tropical Science Center, San Jose, Costa Rica.

Houghton, R. A. (2005), Aboveground Forest Biomass and the Global Carbon Balance, *Glob. Chang. Biol.*, *11*(6), 945–958, doi:10.1111/j.1365-2486.2005.00955.x.

Huntington, T. G. (2006), Evidence for intensification of the global water cycle: Review and synthesis, *J. Hydrol.*, *319*(1-4), 83–95, doi:10.1016/j.jhydrol.2005.07.003.

Jarvis, P. G., and K. G. McNaughton (1986), Stomatal control of transpiration: scaling up from leaf to region, *Adv. Ecol. Res.*, *15*, 1–48.

Jenny, H. (1941), *Factors of Soil Formation*, McGraw-Hill Book Company, New York, NY.

Jeschke, J. M., and D. L. Strayer (2008), Usefulness of bioclimatic models for studying climate change and invasive species, *Ann. N. Y. Acad. Sci.*, *1134*, 1–24, doi:10.1196/annals.1439.002.

Jin, Y., and M. L. Goulden (2013), Ecological consequences of variation in precipitation: separating short- versus long-term effects using satellite data, *Glob. Ecol. Biogeogr.*, n/a–n/a, doi:10.1111/geb.12135.

Keeland, B. D., and P. J. Young (2007), Construction and Installation of Dendrometer Bands for Periodic Tree-Growth Measurements, *USGS Natl. Wetl. Res. Cent.*, 1–8. Available from: http://www.nwrc.usgs.gov/Dendrometer

Keith, H., B. G. Mackey, and D. B. Lindenmayer (2009), Re-evaluation of forest biomass carbon stocks and lessons from the world's most carbon-dense forests, *Proc. Natl. Acad. Sci. U. S. A.*, *106*(28), 11635–11640.

Kelliher, F. M., R. Leuning, and E.-D. Schulze (1993), Evaporation and canopy characteristics of coniferous forests and grasslands, *Oecologia*, *95*, 153–163.

Kelly, A. E., and M. L. Goulden (2008), Rapid shifts in plant distribution with recent climate change, *Proc. Natl. Acad. Sci. U. S. A.*, *105*(33), 11823–6, doi:10.1073/pnas.0802891105.

Kelly, A. E., and M. L. Goulden (2014), Limits on woody biomass and production along a 2300 m elevation gradient, *Prep.*

Kelly, A. E., M. L. Goulden, and A. W. Fellows (2014), A montane Mediterranean climate supports year-round growth and high biomass, *Prep.*

Köppen, W. (1884), Die Warmezonen der Erde, nach der Dauer der heissen, gemassigten und kalten Zeit und nach der Wirkung der Warme auf die organische Welt betrachtet (The thermal zones of the earth according to the duration of hot, moderate and cold periods and to the impac, *Meteorol. Zeitschrift*, *1*, 215–226, doi:10.1127/0941-2948/2011/105.

LaDochy, S., R. Medina, and W. Patzert (2007), Recent Calfornia climate variability: spatial and temporal patterns in temperature trends, *Clim. Res.*, *33*, 159–169.

Law, B. E., M. G. Ryan, and P. M. Anthoni (2008), Seasonal and annual respiration of a ponderosa pine ecosystem, *Glob. Chang. Biol.*, *5*, 169–182.

Lieth, H. (1975), Modeling the primary productivity of the world, edited by H. Lieth and R. Whittaker, *Prim. Product. Biosph.*, *14*, 237–263, doi:10.1007/978-3-642-80913-2_12.

Loarie, S. R., B. E. Carter, K. Hayhoe, S. M. McMahon, R. Moe, C. A. Knight, and D. D. Ackerly (2008), Climate change and the future of California's endemic flora, *PLoS One*, *3*(6), e2502, doi:10.1371/journal.pone.0002502.

Loarie, S. R., P. B. Duffy, H. Hamilton, G. P. Asner, C. B. Field, and D. D. Ackerly (2009), The velocity of climate change, *Nature*, *462*(7276), 1052–1055, doi:10.1038/nature08649.

Van Mantgem, P. J., and N. L. Stephenson (2007), Apparent climatically induced increase of tree mortality rates in a temperate forest, *Ecol. Lett.*, *10*(10), 909–16, doi:10.1111/j.1461-0248.2007.01080.x.

McDowell, N. G. (2011), Mechanisms linking drought, hydraulics, carbon metabolism, and vegetation mortality, *Plant Physiol.*, *155*(3), 1051–9, doi:10.1104/pp.110.170704.

Means, J. E., H. A. Hansen, G. J. Koerper, P. B. Alaback, and M. W. Klopsch (1994), *Software for Computing Plant Biomass - BIOPAK Users Guide*, Portland, OR, OR.

Medvigy, D., S. C. Wofsy, J. W. Munger, and P. R. Moorcroft (2010), Responses of terrestrial ecosystems and carbon budgets to current and future environmental variability, *Proc. Natl. Acad. Sci. U. S. A.*, *107*(18), 8275–80, doi:10.1073/pnas.0912032107.

Merriam, C. H. (1894), Laws of Temperature Control of the Geographic Distribution of Terrestrial Animals and Plants, *Natl. Geogr. Mag.*, *6*, 229–238.

Millar, C. I., R. D. Westfall, and D. L. Delany (2007), Response of high-elevation limber pine (Pinus flexilis) to multiyear droughts and 20th-century warming, Sierra Nevada, California, USA, *Can. J. For. Res.*, *37*(12), 2508–2520, doi:10.1139/X07-097.

Moffat, A. M. et al. (2007), Comprehensive comparison of gap-filling techniques for eddy covariance net carbon fluxes, *Agric. For. Meteorol.*, *147*(3-4), 209–232, doi:10.1016/j.agrformet.2007.08.011.

Monteith, J. L. (1965), Evaporation and environment, *Soc. Exp. Biol. Symp.*, *19*, 205–234.

National Atmospheric Deposition Program (2013), NADP/NTN Monitoring Location CA28, *Natl. Atmos. Depos. Progr.* Available from: http://nadp.sws.uiuc.edu/sites/siteinfo.asp?id=CA28&net=NTN (Accessed 1 May 2013)

Nobel, P. S., and P. W. Jordan (1983), Transpiration stream of desert species: resistances and capacitances for a C3, a C4 and a CAM plant, *J. Exp. Bot.*, *34*(147), 1379–1391.

Oak Ridge National Laboratory Distributed Active Archive Center (ORNL DAAC) (2011), MODIS Terra 15A2, Available from: http://daac.ornl.gov/MODIS/modis.html (Accessed 28 January 2014)

Osmond, C. B., M. P. Austin, J. A. Berry, W. D. Billings, J. S. Boyer, J. W. H. Dacey, P. S. Nobel, S. D. Smith, and W. E. Winner (1987), Stress Physiology and the Distribution of Plants, *Bioscience*, *37*(1), 38–48, doi:10.2307/1310176.

Panek, J. A., and A. H. Goldstein (2001), Response of stomatal conductance to drought in ponderosa pine: implications for carbon and ozone uptake, *Tree Physiol.*, *21*(5), 337–44.

Parker, J. (1963), Cold resistance in woody plants, *Bot. Rev.*, *29*(2), 124–163.

Parmesan, C. (2006), Ecological and Evolutionary Responses to Recent Climate Change, *Annu. Rev. Ecol. Evol. Syst.*, *37*(1), 637–669, doi:10.1146/annurev.ecolsys.37.091305.110100.

Parmesan, C., and G. Yohe (2003), A globally coherent fingerprint of climate change impacts across natural systems, *Nature*, *421*(6918), 37–42, doi:10.1038/nature01286.

Piao, S. et al. (2008), Net carbon dioxide losses of northern ecosystems in response to autumn warming, *Nature*, *451*(7174), 49–52, doi:10.1038/nature06444.

Potter, C. S. (2010), The carbon budget of California, *Environ. Sci. Policy*, *13*(5), 373–383, doi:10.1016/j.envsci.2010.04.008.

Potter, C. S., J. T. Randerson, C. B. Field, P. A. Matson, P. M. Vitousek, H. A. Mooney, and S. A. Klooster (1993), Terrestrial ecosystem production: A process model based on global satellite and surface data, *Global Biogeochem. Cycles*, *7*(4), 811–841.

PRISM Climate Group (2013), PRISM Gridcell Time-Series, *Oregon State Univ.* Available from: http://prismmap.nacse.org/nn/ (Accessed 1 May 2013)

Rambo, T. R., and M. P. North (2009), Canopy microclimate response to pattern and density of thinning in a Sierra Nevada forest, *For. Ecol. Manage.*, *257*(2), 435–442, doi:10.1016/j.foreco.2008.09.029.

Raven, P. H., and D. I. Axelrod (1995), *Origin and Relationships of the California Flora*, California Native Plant Society, Sacramento, CA.

Roderick, M. L., and G. D. Farquhar (2002), The cause of decreased pan evaporation over the past 50 years, *Science (80-.).*, (298), 1410–1412, doi:10.1126/science.1075390-a.

Rosenzweig, M. L. (1968), Net Primary Productivity of Terrestrial Communities: Prediction from Climatological Data, *Am. Nat.*, *102*(923), 67–74.

Royce, E. B., and M. G. Barbour (2001a), Mediterranean climate effects. I. Conifer water use across a Sierra Nevada ecotone, *Am. J. Bot.*, *88*(5), 919–932.

Royce, E. B., and M. G. Barbour (2001b), Mediterranean climate effects. II. Conifer growth phenology across a Sierra Nevada ecotone, *Am. J. Bot.*, *88*(5), 919–932.

Running, S. W., P. E. Thornton, R. R. Nemani, and J. M. Glassy (2000), Global Terrestrial Gross and Net Primary Productivity from the Earth Observing System, in *Methods in Ecosystem Science*, edited by O. E. Sala, R. B. Jackson, H. A. Mooney, and R. W. Howarth, pp. 44–57, Springer-Verlag, New York.

Ryan, M. G., and R. H. Waring (1992), Maintenance respiration and stand development in a subalpine lodgepole pine forest, *Ecology*, *73*(6), 2100–2108.

Ryan, M. G., S. T. Gower, R. M. Hubbard, R. H. Waring, H. L. Gholz, W. P. Cropper Jr., and S. W. Running (1995), Woody tissue maintenance respiration of four conifers in contrasting climates, *Oecologia*, *101*, 133–140.

Sage, R. F., and R. W. Pearcy (1987), The nitrogen use efficiency of C3 and C4 Plants, *Plant Physiol.*, *84*, 959–963.

Schoenherr, A. A. (1992), Sierra Nevada, in *A Natural History of California*, edited by P. Faber and B. M. Pavlik, p. 772, University of California Press, Berkeley, CA.

Scholze, M., W. Knorr, N. W. Arnell, and I. C. Prentice (2006), A climate-change risk analysis for world ecosystems, *Proc. Natl. Acad. Sci. U. S. A.*, *103*(35), 13116–20, doi:10.1073/pnas.0601816103.

Sharkey, T. D. (1984), Transpiration-induced changes in the photosynthetic capacity of leaves, *Planta*, *160*(2), 143–150, doi:10.1007/BF00392862.

Stephenson, N. L. (1988), Climatic control of vegetation distribution: The role of the water balance with examples from North America and Sequoia National Park, California, 315 pp., Cornell University.

Stephenson, N. L. (1998), Actual evapotranspiration and deficit: biologically meaningful correlates of vegetation distribution across spatial scales, *J. Biogeogr.*, *25*, 855–870.

Stephenson, N. L., and P. J. Van Mantgem (2005), Forest turnover rates follow global and regional patterns of productivity, *Ecol. Lett.*, *8*(5), 524–31, doi:10.1111/j.1461-0248.2005.00746.x.

Stephenson, N. L., P. J. van Mantgem, A. G. Bunn, H. Bruner, M. E. Harmon, K. B. O'Connel, D. L. Urban, and J. F. Franklin (2012), Causes and implications of the correlation between forest productivity and tree mortality rates, *Ecol. Monogr.*

Stewart, I. T., D. R. Cayan, and M. D. Dettinger (2005), Changes toward earlier streamflow timing across western North America, *J. Clim.*, *18*, 1136–1156.

Stewart, J. B. (1988), Modelling surface conductance of pine forest, *Agric. For. Meteorol.*, *43*(1), 19–35, doi:10.1016/0168-1923(88)90003-2.

Thornthwaite, C. W. (1948), An approach toward a rational classification of climate, *Geogr. Rev.*, *38*(1), 55–94.

Trujillo-Gomez, E., N. P. Molotch, M. L. Goulden, A. E. Kelly, and R. C. Bales (2012), Elevation-dependent influence of snow accumulation on forest greening, *Nat. Geosci.*, *5*(10), 705–709, doi:10.1038/ngeo1571.

Turnipseed, A. A., P. D. Blanken, D. E. Anderson, and R. K. Monson (2002), Energy budget above a high-elevation subalpine forest in complex topography, *Agric. For. Meteorol.*, *110*(3), 177–201, doi:10.1016/S0168-1923(01)00290-8.

Twine, T. E., W. P. Kustas, J. M. Norman, D. R. Cook, P. R. Houser, T. P. Meyers, J. H. Prueger, P. J. Starks, and M. L. Wesely (2000), Correcting eddy-covariance flux underestimates over a grassland, *Agric. For. Meteorol.*, *103*(3), 279–300, doi:10.1016/S0168-1923(00)00123-4.

Urban, D. L., C. Miller, P. N. Halpin, and N. L. Stephenson (2000), Forest gradient response in Sierran landscapes: the physical template, *Landsc. Ecol.*, *15*, 603–620.

USDA (2009), *Soil Survey Geographic (SSURGO) database for Sierra National Forest Area, Parts of Fresno, California*, Fort Worth, TX.

Walker, R., M. Rosenberg, R. Warbington, B. Schwind, D. Beardsley, C. Ramirez, L. Fischer, and B. Frerichs (2004), *Inventory of tree mortality in Southern California mountains (2001-2004) due to bark beetle impacts*.

Walter, H., and S.-W. Breckle (2002), *Walter's Vegetation of Earth: The ecological systems of the geobiosphere*, 4th ed., Springer-Verlag, Berlin.

Waring, R. H., and J. F. Franklin (1979), Evergreen coniferous forests of the Pacific Northwest, *Science (80-.).*, *204*(4400), 1380–1386.

Whittaker, R. H., and W. A. Niering (1975a), Vegetation of the Santa Catalina Mountains , Arizona. V. Biomass , Production , and Diversity along the Elevation Gradient, *Ecology*, *56*(4), 771–790.

Whittaker, R. H., and W. A. Niering (1975b), Vegetation of the Santa Catalina Mountains, Arizona: A gradient analysis of the south slope, *Ecology*, *56*(4), 771–790.

Whittaker, R. H., S. A. Levin, and R. B. Root (1973), Niche, habitat, and ecotope, *Am. Nat.*, *107*(955), 321–338.

Williams, A. P. et al. (2012), Temperature as a potent driver of regional forest drought stress and tree mortality, *Nat. Clim. Chang.*, *3*(3), 292–297, doi:10.1038/nclimate1693.

Williams, J. W., and S. T. Jackson (2007), Novel climates, no-analog communities, and ecological surprises, *Front. Ecol. Environ.*, *5*(9), 475–482, doi:10.1890/070037.

Williams, J. W., S. T. Jackson, and J. E. Kutzbach (2007), Projected distributions of novel and disappearing climates by 2100 AD, *Proc. Natl. Acad. Sci. U. S. A.*, *104*(14), 5738–5742, doi:10.1073/pnas.0606292104.

Wilson, K. B., P. J. Hanson, P. J. Mulholland, D. D. Baldocchi, and S. D. Wullschleger (2001), A comparison of methods for determining forest evapotranspiration and its components: sap-flow , soil water budget , eddy covariance and catchment water balance, *Agric. For. Meteorol.*, *106*(2001), 153–168.

Wilson, K. B. et al. (2002), Energy balance closure at FLUXNET sites, *Agric. For. Meteorol.*, *113*(1-4), 223–243, doi:10.1016/S0168-1923(02)00109-0.

Winograd, I. J., A. C. Riggs, and T. B. Coplen (1998), The relative contributions of summer and cool-season precipitation to groundwater recharge, Spring Mountains, Nevada, USA, *Hydrogeol. J.*, *6*(1), 77–93, doi:10.1007/s100400050135.

Yuan, W. et al. (2011), Thermal adaptation of net ecosystem exchange, *Biogeosciences*, *8*(6), 1453–1463, doi:10.5194/bg-8-1453-2011.